AGU PUBLICATIONS

JGR

Journal of Geophysical Research: Oceans

RESEARCH ARTICLE

10.1002/2015JC010762

Multidecadal variability of potential temperature, salinity, and transport in the eastern subpolar North Atlantic

N. P. Holliday[1], S. A. Cunningham[2], C. Johnson[2], S. F. Gary[2], C. Griffiths[2], J. F. Read[1], and T. Sherwin[2]

[1]National Oceanography Centre, Southampton, UK, [2]Scottish Association for Marine Science, Oban, Scotland

Key Points:
- Extended Ellett Line is an exceptionally long-time series of deep-ocean data
- Upper ocean varies by ±0.06°C and ±0.08 in salinity over 4 decades
- Highest overturning in Iceland Basin, greatest variability in Rockall Trough

Correspondence to:
N. P. Holliday,
penny.holliday@noc.ac.uk

Citation:
Holliday, N. P., S. A. Cunningham, C. Johnson, S. F. Gary, C. Griffiths, J. F. Read, and T. Sherwin (2015), Multidecadal variability of potential temperature, salinity, and transport in the eastern subpolar North Atlantic, *J. Geophys. Res. Oceans*, *120*, 5945–5967, doi:10.1002/2015JC010762.

Received 4 FEB 2015
Accepted 10 AUG 2015
Accepted article online 13 AUG 2015
Published online 4 SEP 2015

Abstract The Extended Ellett Line (EEL) hydrographic section extends from Scotland to Iceland crossing the Rockall Trough, Hatton-Rockall Basin, and Iceland Basin. With 61 full-depth stations at a horizontal resolution of 10–50 km, the EEL samples the upper limb of the Atlantic Meridional Overturning Circulation flowing across the Iceland-Scotland Ridge into the Nordic Seas. The Rockall Trough has been sampled nearly four times per year from 1975 to 1996, and the full section annually since 1996. The EEL is an exceptionally long-time series of deep ocean temperatures and salinities. This study extends prior work in the Rockall Trough, and examines for the first time 18 year records in the Iceland and Hatton-Rockall Basins. We quantify errors in the time series from two sources: observational errors and aliasing. The data quality and annual sampling are suitable for observing interannual to decadal variability because the variability exceeds our error estimates. The upper waters of all three basins are cooler/fresher from 1997 to 2001, warmer/more saline 2001–2006, and cooler/fresher from 2006 to 2014. A reference level for geostrophic shear is developed heuristically and by comparison with sea-surface altimetry. The mean northward transport in the upper waters is 6.7 ± 3.7 Sv and there is a 6.1 ± 2.5 Sv southward flow below the thermocline. Although the magnitude of the Iceland Basin overturning circulation (4.3 ± 1.9 Sv) is greater than in the Rockall Trough (3.0 ± 3.7 Sv), the variability is greater in the Rockall Trough. We discuss the results in the context of our understanding of drivers of variability.

1. Introduction

The upper waters in the eastern subpolar North Atlantic (above the permanent thermocline at 500–1000 dbar) either enter the Arctic Ocean, or are incorporated into North Atlantic Deep Water and exported from the Labrador Sea as the lower limb of the Atlantic Meridional Overturning Circulation (AMOC). The supply of warm and salty water to the Arctic and deep water formation areas provides an important feedback between the oceans and atmosphere, and is therefore a key aspect of the climate system. There is evidence that the anomalies formed in the subpolar North Atlantic persist into the surface Nordic Seas, the subsurface Arctic, and the deep return layer of the AMOC [*Glessmer et al.*, 2014; *Polyakov et al.*, 2011; *Eldevik et al.*, 2009]. Thus variations of thermohaline properties in the eastern subpolar gyre on climate time scales need to be quantified and understood.

Of the upper waters that enter the subpolar gyre, it is estimated that around 60% recirculates within the North Atlantic. Of this 12.7 Sv of recirculating water, 10.2 Sv is incorporated into the lower limb of the AMOC [*Sarafanov et al.*, 2012] after gaining density through air-sea fluxes, mixing, and convection. An estimated 7.5 Sv of Atlantic Water in the subpolar gyre, however, flows northward over the Greenland-Scotland Ridge into the Nordic Seas. The majority (90 %) of this inflow is to the east of Iceland [*Hansen et al.*, 2003; *Turrell et al.*, 2003; *Jonsson and Briem*, 2003]. Around 3.0 Sv of the inflow to the Nordic Seas continues northward contributing to the subsurface Atlantic Water layer of the Arctic Ocean [*Beszczynska-Moller et al.*, 2012], while the remaining 4.5 Sv recirculates within the Nordic Seas. This recirculating water, which enters areas of dense water formation, returns southward to the subpolar North Atlantic as 6–7 Sv of overflow water over the Greenland-Scotland Ridge [*Hansen and Østerhus*, 2000; *Sarafanov et al.*, 2012].

While buoyancy fluxes are not thought necessary for the existence of the AMOC, they are important for controlling its strength and structure [e.g., *Cunningham and Marsh*, 2010]. Salinity advection feedbacks suggest that two stable circulations are possible [*Stommel*, 1961] and recent observations indeed indicate that the AMOC can exist in two states [*Bryden et al.*, 2011]. Thus the question of buoyancy forcing, through the

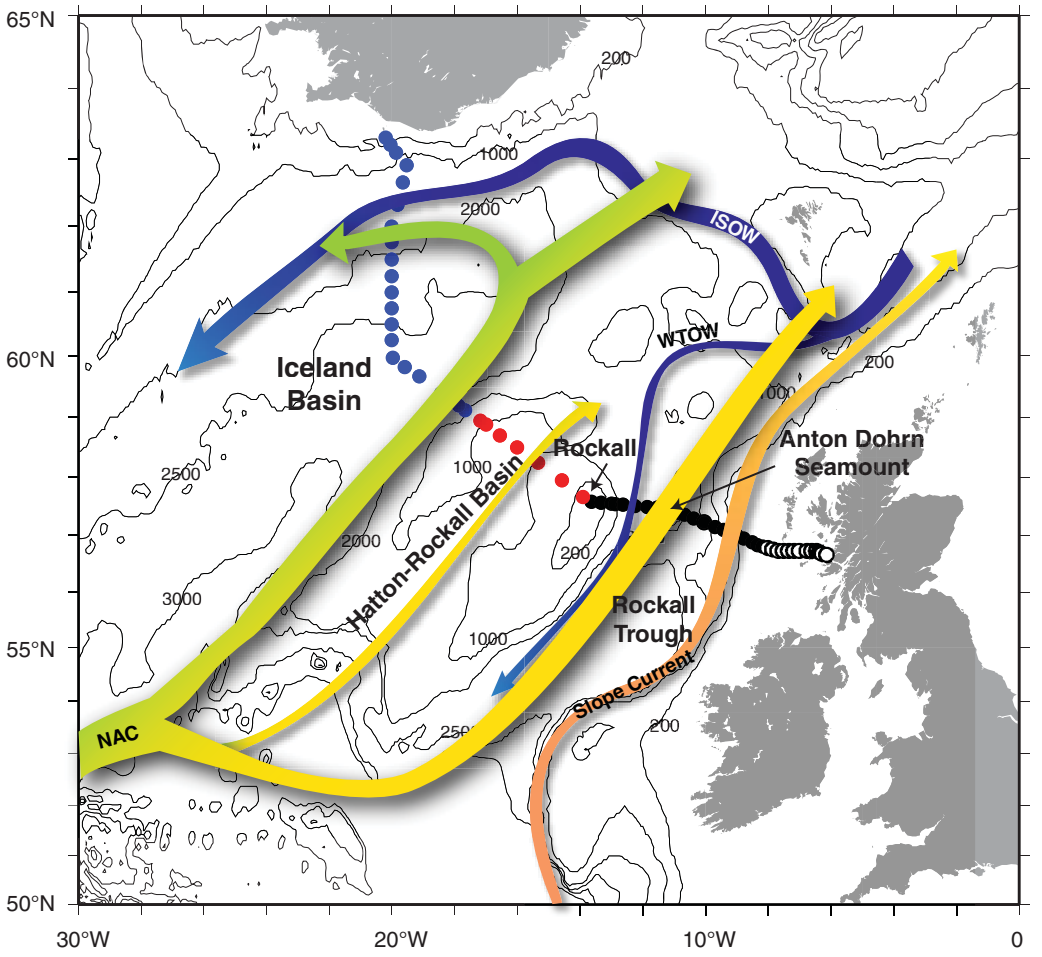

Figure 1. The location of the Extended Ellett Line and schematic of primary upper ocean (0 to ~1000m) and deep current pathways. Dots represent the position of standard stations; from 1975 to 1996 the program occupied the stations in the Rockall Trough (black) and European continental shelf (white), and from 1997 onward the Hatton-Rockall Basin (red) and the Iceland Basin (blue) stations were also sampled. Not all sections completed all stations, and station positions may vary slightly from cruise to cruise. The colored arrows indicate the main pathways of the major currents in the upper ocean (slope current and North Atlantic Current, NAC) and the deep ocean (Iceland-Scotland Overflow Water, ISOW, and Wyville-Thomson Overflow Water, WTOW). The color range from orange to green in the upper ocean currents indicates an east-to-west and north-to-south decrease in salinity and temperature of the mode waters. Intermediate water (Labrador Sea Water) circulates cyclonically in the deep basins but is not shown here.

supply of warm and salty water from the Atlantic to high latitudes in the deep-water formation regions, is of central importance to the future evolution of the AMOC.

The Rockall Trough, through UK marine research programs, has been observed for over seven decades. The first measurements were of surface temperature and salinity by Ocean Weather Ships, with a program of sustained observations from research ships from 1975 onward. More recently this has been supplemented by data from autonomous vehicles [*Holliday and Cunningham*, 2013]. Now known as the Extended Ellett Line (EEL, Figure 1), the section is located between Scotland and Iceland running close to the northern boundaries of the Rockall Trough, Hatton-Rockall Basin, and Iceland Basin. These measurements have provided an exceptionally rare record of high-quality temperature and salinity data on this full-depth open-ocean section.

In the area sampled by the EEL, there is approximately a three-layer circulation (Figure 1). Warm and salty upper water flows in a general north-eastward direction at depths shallower than the thermocline which is typically 500–1000 dbar [*Pollard et al.*, 2004; *Brambilla and Talley*, 2008]. The main center of the cyclonic recirculation within the subpolar gyre is located southwest of the EEL position [*Lavender et al.*, 2005]. At intermediate depths, Labrador Sea Water cyclonically recirculates both within the Iceland Basin and Rockall

Trough [e.g., *Holliday et al*., 2000; *Lankhorst and Zenk*, 2006]. Finally, Iceland-Scotland Overflow Water flows westward/south-westward along the Iceland-Faroes Ridge and Reykjanes Ridge in the Iceland Basin [*Read*, 2001; *Saunders*, 1996]; while a relatively small amount of Wyville Thomson Ridge Overflow Water flows southward in the western Rockall Trough at densities $>$27.70 kg m^{-3} [*Johnson et al*., 2010]. Other water masses such as Subarctic Intermediate Water and Mediterranean Outflow Water influence the section but to a lesser extent.

Water mass properties and volume transport in the Rockall Trough have previously been described as having multiyear variability with changes of $\pm$0.04 in salinity in the upper ocean (0–1000 dbar) and $\pm$0.02 in the deep ocean ($>$1200 dbar) between 1975 and 1998 [*Holliday et al*., 2000]. Salinity and temperatures have increased significantly since the mid-1990s [*Holliday et al*., 2008; *Hughes et al*., 2012]. These latter changes in the eastern margin of the subpolar gyre have been attributed to a greater influence of subtropical water as the subpolar gyre circulation slowed and the subpolar front moved westward [*Holliday*, 2003; *Hatun et al*., 2004; *Hakkinen and Rhines*, 2004]. Recently a study of nutrient concentrations suggested that the eastern subpolar gyre reached the maximum potential influence of subtropical waters around the mid-2000s, and that subsequently other drivers of variability have become more important [*Johnson et al*., 2013].

In this study, we present data from nearly 40 years of hydrographic measurements in the Rockall Trough, extending the previously published time series of *Holliday et al*. [2000] by 16 years. Additionally, 18 years of new data in the Iceland Basin and Hatton-Rockall Basin are analyzed. We quantify errors in the time series from two sources that affect the interpretation of interannual to decadal variability: observational errors and aliasing of intra-annual variability to lower frequencies. For the first, we use the stable thermocline water mass as the basis for assessing inter-cruise data quality, while for the second we use a high-resolution forced numerical model to develop statistics of intra-annual variability. We calculate the mean geostrophic circulation and its variability over the last 18 years. The reference level for the circulation is developed heuristically and by numerical comparison with AVISO absolute sea surface heights. Finally, we discuss the observed variability of surface, intermediate, and deep waters in the context of present-day understanding of drivers of variability.

2. Resources: Data and Model

2.1. Potential Temperature and Salinity Data From the Extended Ellett Line

The Extended Ellett Line has been occupied 1–4 times per year since 1975 (Table 1 lists the cruises used in this analysis). The core data set (available from the British Oceanographic Data Centre, www.bodc.ac.uk) consists of pressure, potential temperature, and salinity from CTDs (STDs prior to 1978), with the addition of dissolved oxygen and nutrient samples since 1996. The physical data, which are the focus of this study, have varying quality; since 1996, the CTD data have been calibrated and documented to meet international repeat hydrography standards (www.go-ship.org, potential temperature accurate to at least 0.002°C, salinity accurate to 0.001), but data quality was generally lower prior to that. For 10 pre-1996, occupations data quality is poor; these are excluded from the analysis [*Holliday et al*., 2000]. We quantify the uncertainty due to data quality in the remaining data sets in section 3.

The nominal station spacing for the section is 30 km in the Iceland Basin, 30–50 km through the Hatton-Rockall Basin, 20 km in the Rockall Trough, and 10 km on the Scottish continental shelf (Figure 1). Station spacing decreases over the sloping topography of the continental shelves. From 1975 to 1996, the Ellett Line stretched from the Scottish coast to the island of Rockall; in 1997 and subsequent years, the section was extended through the Hatton-Rockall and Iceland Basins to the coast of Iceland. For simplicity, throughout this manuscript, we will refer to all the sections as the Extended Ellett Line (EEL).

The EEL lies under the North Atlantic storm track and is well known for presenting challenges for ship-based data collection at all times of the year. Few of the EEL occupations have managed to complete all the standard stations shown in Figure 1. In the early part of the time series, when the section was restricted to the Rockall Trough, there were sections taken throughout the year, though rarely in December and January. Since 1996, the cruises have largely been scheduled for spring or summer, leading to an increased number of completed sections, but a greatly reduced sampling of the annual cycle. A winter cruise was attempted in February 2000 (*RRS Discovery* D245), but high winds and extreme waves were recorded [*Holliday et al*., 2006] and few CTDs were completed. Recently, observations of the EEL during the winter have been started

Table 1. List of Ellett Line (1975–1996) and Extended Ellett Line (1997 Onward) Cruises Used in the Analysis

Cruise	Year	Month
C775	1975	May
C1075	1975	Jul
C1475	1975	Nov
C576	1976	Apr
C876	1976	May
C477	1977	Mar
C677	1977	Apr
C1377	1977	Aug
C678	1978	Apr
C978	1978	Jun
C11B78	1978	Aug
C11D78	1978	Sept
C1478	1978	Nov
C779	1979	May
C1379	1979	Sept
C1679	1979	Oct
C780	1980	May
C281	1981	Jan
C681	1981	Apr
C1081	1981	Jul
C1581	1981	Oct
C783	1983	May
C1183	1983	Aug
C1084	1984	Nov
C185	1985	Jan
C485	1985	May
C885	1985	Aug
C987	1987	Jan
C1487	1987	Apr
C3088	1988	Jun
D180	1989	Jan
LF189	1989	May
LF289	1989	Aug
CD44	1989	Nov
C67	1990	Jun
C71	1990	Sep
C97	1992	Sep
C103	1993	May
C105	1993	Sep
C110	1994	Mar
C112	1994	May
C114	1994	Aug
C120	1995	Aug
C124	1996	Jan
D223	1996	Oct
D230[a]	1997	Sep
D233[a]	1998	May
D242[a]	1999	Sep
D245	2000	Feb
SC0700	2000	Apr
D253[a]	2001	May
SC0703	2003	Apr
P300	2003	Jul
P314[a]	2004	Jul
CD176	2005	Oct
D312	2006	Oct
D321	2007	Aug
SC08	2008	May
D340[a]	2009	Jun
D351[a]	2010	May
D365[a]	2011	May
D379[a]	2012	Aug
JC086[a]	2013	May
JR302[a]	2014	Jul

[a]Indicates cruises that completed the full Iceland to Scotland section and are used in the calculation of mean sections and geostrophic velocities.

with gliders and as the number of winter sections increases, analysis of the seasonal cycle of the EEL will be presented elsewhere.

For the purpose of this study, the section is subdivided into three segments based on topography (Figure 1). The Iceland Basin stations are located between Iceland and the shallowest station on the Hatton Bank; the Hatton-Rockall Basin stations are between the Hatton Bank and the Rockall Plateau; and the Rockall Trough stations are defined from the shallowest station on the Rockall Plateau to a station just past the continental shelf break at 130 m water depth. Stations inshore of the 130 m isobath are classed as shelf stations and are excluded from this study since their variability has recently been analyzed [*Inall et al.*, 2009].

For section 3, we compute mean sections of potential temperature, salinity, and potential density as follows. Data from 11 EEL cruises between 1997 and 2014 (Table 1) were interpolated onto a standard vertical (10 dbar) and horizontal grid (10 km), and the mean and standard deviation of potential temperature, salinity, and potential density for each data point calculated. Only near complete sections were used to ensure even sampling of the deep ocean, particularly over sloping bathymetry. Therefore, data between 2005 and 2007 were not used, as bad weather meant that several stations could not be occupied. It should be noted that as cruises were between May and September only, all mean sections represent the summer features.

Additionally we divide the water column into layers defined as density ranges (Table 2). The density boundaries were determined by examining the hydrographic structure (Figures 2–4) and the potential temperature-salinity relationship of the section (Figure 5). We reduce bias and aliasing introduced by the undersampling of the seasonal cycle by excluding the summer seasonally warmed surface layer. A range of isopycnals were tested to define the upper limit of the upper ocean water, with the 27.20 kg m^{-3} isopycnal found to best capture most of the volume of the upper ocean whilst excluding the summer surface layer (0 to maximum of 150 dbar).

The permanent thermocline is defined as water with densities between 27.50 and 27.70 kg m^{-3} with the upper limit lying below the coolest and freshest varieties of upper waters of the Iceland Basin (Figures 2 and 3). Using the 27.50 kg m^{-3} isopycnal as the lower limit does mean that sometimes a small amount of thermocline water is included in the upper ocean class for the Hatton-Rockall Basin and Rockall Trough (Figure 2).

The LSW is defined as being within the density range 27.70–27.85 kg m^{-3}, and the densest layer is water below that (Figures 2–4). In the literature, the densest water of

Table 2. Definitions of Water Column Layers Based on Potential Density Ranges

Layer Name	Potential Density Range
Seasonally warmed surface layer	<27.20 kg m^{-3}
Upper ocean	27.20–27.50 kg m^{-3}
Permanent thermocline or pycnocline	27.50–27.70 kg m^{-3}
Intermediate water (Labrador Sea Water)	27.70–27.85 kg m^{-3}
Overflow water	>27.85 kg m^{-3}

the Iceland Basin (Iceland-Scotland Overflow Water) is sometimes defined as having a density greater than 27.80 kg m^{-3} [e.g., *Kanzow and Zenk*, 2014], and a recent study [*Sarafanov et al.*, 2012] defined it as being greater than 27.88 kg m^{-3}. We recognize that there is a mixing line between LSW and ISOW in this location (Figure 5) and choosing a single isopycnal is making a somewhat artificial distinction between the two water types. However, we choose 27.85 kg m^{-3} as being most consistent with the potential temperature-salinity distribution shown in Figure 5. It should be noted that the LSW definition may include less dense components of ISOW and the implications of the definition are discussed later.

2.2. The FLAME Model

The ocean general circulation model output used in this study is the eddy-resolving configuration of the Family of Linked Atlantic Modelling Experiments (FLAME) [*Böning et al.*, 2006]. This regional model output, stored

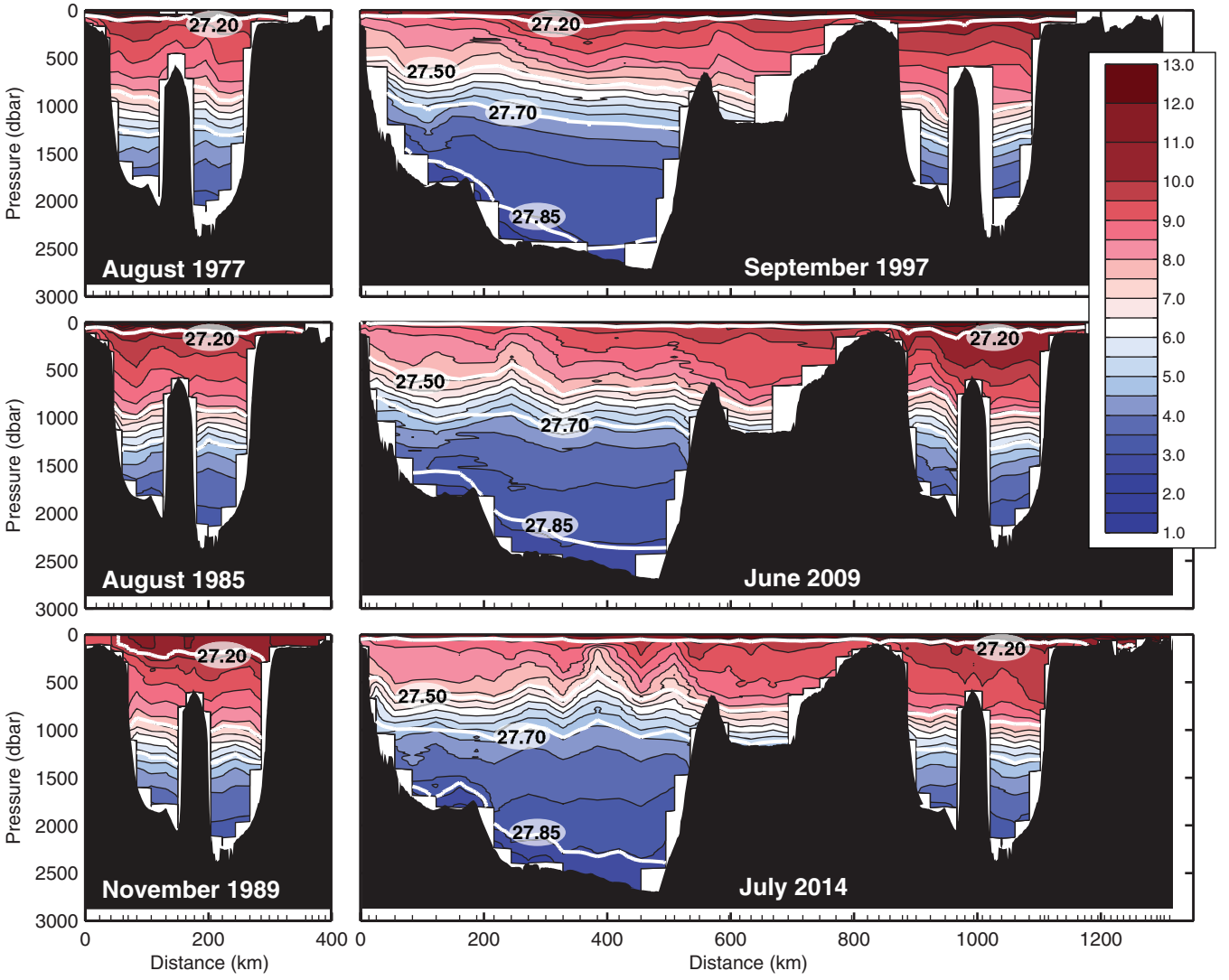

Figure 2. Example potential temperature sections from the Extended Ellett Line time series. The sections in the left column are earlier, shorter sections between Rockall (left) and Scotland. The sections in the right column are later extended sections from Iceland (left) to Scotland. Isopycnals shown as bold, white lines. Black shading indicates bathymetry. Tick marks on horizontal axes indicate the CTD station positions.

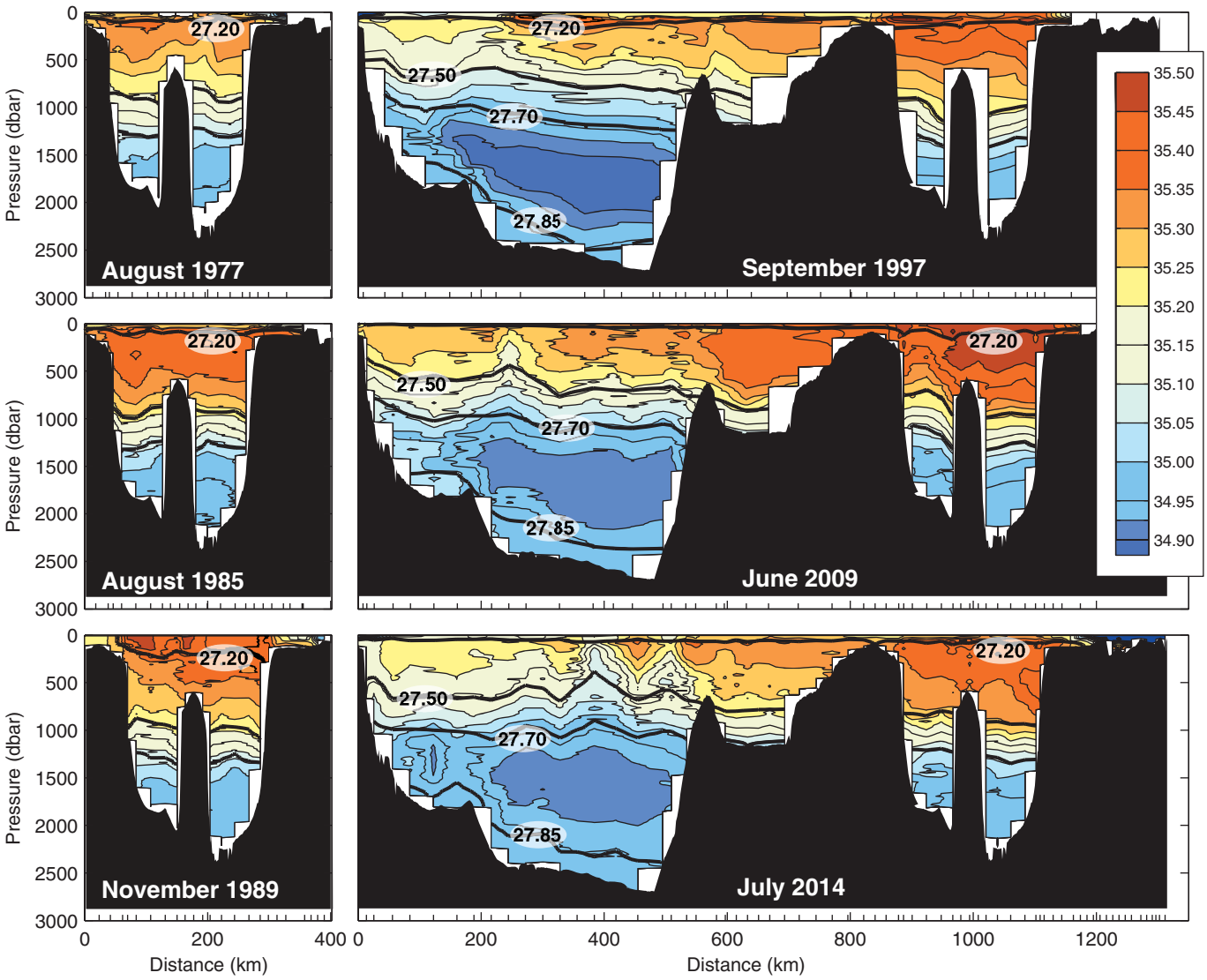

Figure 3. Example salinity sections from the Extended Ellett Line time series corresponding to the temperature sections in Figure 2. Isopycnals shown as bold, black lines. Black shading indicates bathymetry. Tick marks on horizontal axes indicate the CTD station positions.

in 3 day snapshots of potential temperature, salinity, and velocity, has been shown to compare favorably with observations of the large-scale eddy activity, density structure, and pathways of the shallow [*Burkholder and Lozier*, 2011] and deep [*Gary et al.*, 2011] limbs of the AMOC as well as the North Atlantic Subtropical Mode Water [*Gary et al.*, 2014]. As this model has been described in other publications, only a brief summary is provided here. The model grid has a resolution of 1/12° that spans 18°S–70°N over the width of the Atlantic Ocean and open boundary conditions at the north and south. There are 45 z-levels in the vertical with grid spacing transitioning from 10 m at the surface to 250 m at depth. A bottom boundary layer [*Beckmann and Döscher*, 1997] was implemented to minimize spurious mixing over rough topography. The model was spun-up for 10 years with climatological forcing based on the European Centre for Medium Range Weather Forecasts (ECMWF) reanalysis. After spin-up, the model was forced with interannual anomalies based on the National Centers for Environmental Prediction/National Center for Atmospheric Research (NCEP/NCAR) reanalysis from 1990 to 2004 [*Kalnay et al.*, 1996] superimposed onto the initial ECMWF climatological forcing. Since the EEL does not correspond exactly to model grid nodes, the model fields were linearly interpolated at each snapshot and each z-level onto a list of positions along the EEL spaced evenly at every 1/12°. Time series of model potential temperature and salinity were derived from this model EEL section similarly to the way the observed time series were computed from hydrographic sections.

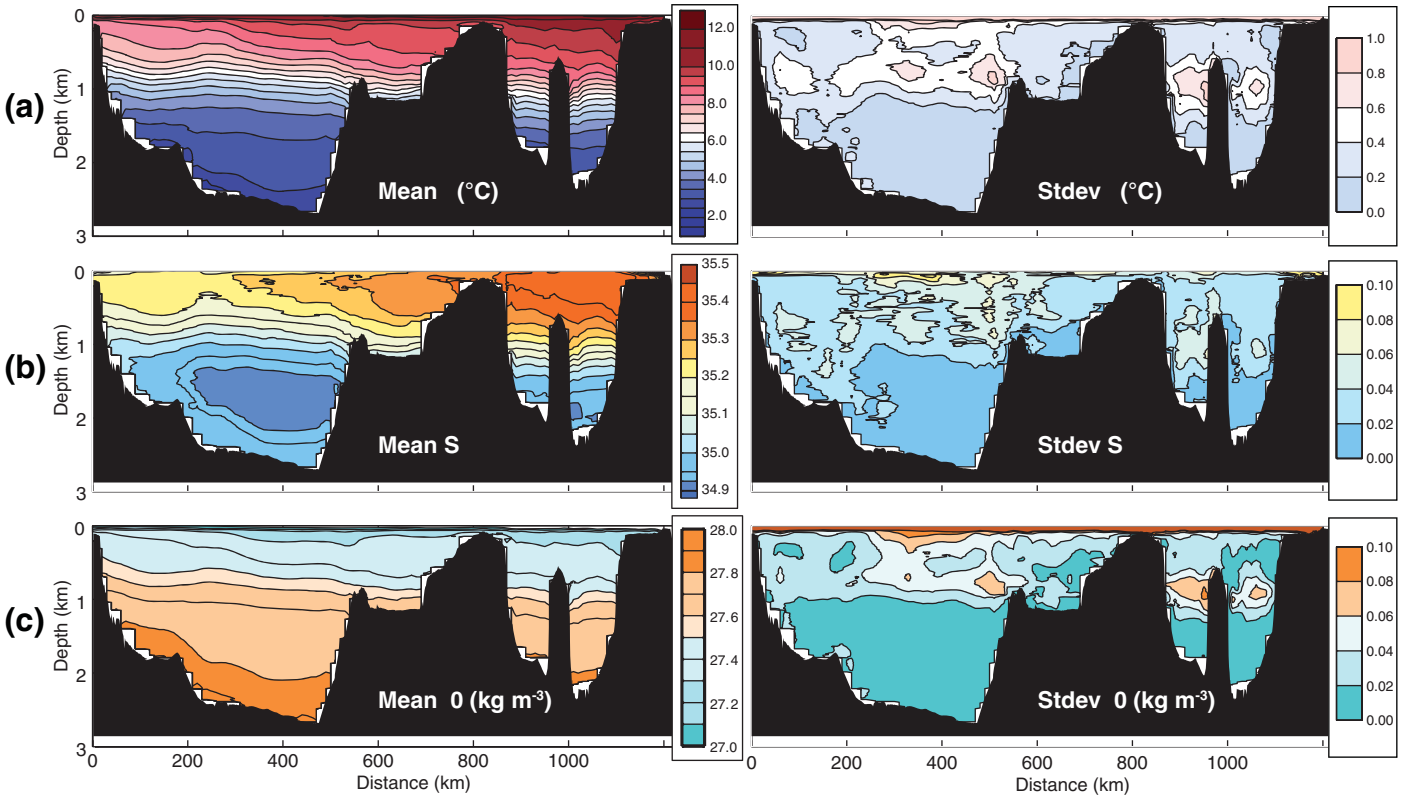

Figure 4. Mean sections across the Extended Ellett Line and associated standard deviations for (a) potential temperature (°C), (b) salinity, and (c) potential density (kg m^{-3}). Fields calculated from 11 complete occupations between 1997 and 2014 (Table 1).

2.3. Satellite Altimetry Data

In order to calculate absolute geostrophic velocities, a level of no/known motion must be assumed. In this work (presented in section 4), we use the DUACS 2014 (V15.0) Ssalto/Duacs multimission altimeter product to help with the determination of this reference level. The product is distributed by *Aviso* with support from *CNES*, and was downloaded as global daily maps of absolute dynamic topography on a 0.25° spatial grid (www.aviso.altimetry.fr). Sea surface dynamic topography is the sum of sea level anomalies and a mean dynamic topography, both referenced over a 20 year period (1993–2012). Key improvements in this new data set are the use of an improved mean dynamic topography (MDT_CNES_CLS13) calculated from GOCE satellite data and in situ observations, and more accurate mapping of the mesoscale [*Rio et al.*, 2011]. The geoid model developed from the GOCE satellite data has a horizontal resolution of 125 km. A multivariate objective analysis (including wind and in situ data) is used to improve the large-scale solution (for heights and velocities), resulting in a final horizontal resolution of 0.25°. In the subpolar North Atlantic, the spatial resolution is therefore approximately 15 km in the longitude direction and 28 km in the latitude direction.

3. Temporal Variability of Potential Temperature and Salinity

3.1. The Hydrography and Spatial Variability of the Eastern Subpolar Region

The basic structure of the hydrography observed by the EEL remains consistent over the length of the time series. The sections in Figures 2 and 3 illustrate some typical conditions observed in the Rockall Trough before 1997, and between Iceland and Scotland after 1997. In all six of these sections, the upper ocean is characterized by warm, saline water (7–13°C, 35.10–35.45), seen also in mean sections calculated from the data from 1997 to 2014 (Figure 4). The upper ocean is consistently warmest, most saline, and deepest in the eastern Rockall Trough (>9.5°C, >35.4 and up to 1000 dbar), becoming progressively cooler, fresher, and shallower toward the northwest. Figure 4 shows that the upper ocean is formed of a series of water types (subpolar mode waters) separated by frontal zones; for example, the mode water with a mean density of

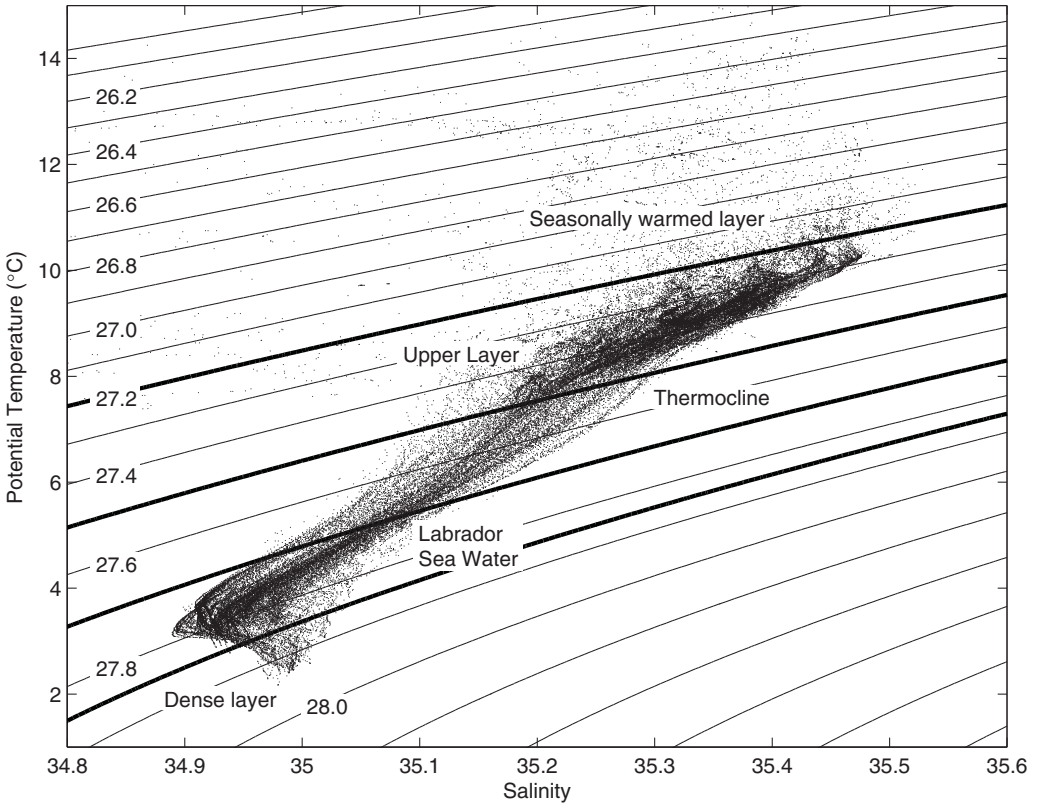

Figure 5. Potential temperature vs salinity range from Extended Ellett Line occupations. Half the cruise data sets are overlaid, to illustrate the full range of properties at all depths from 1975 to 2014. Isopycnals used to define vertical layers in the text are highlighted as bold lines (27.20, 27.50, 27.70, and 27.85 kg m^{-3}).

27.4–27.5 kg m^{-3} in the north Iceland Basin is separated from the mode water density 27.3–27.4 kg m^{-3} in the Hatton-Rockall Basin by the wide frontal region of the North Atlantic Current. The frontal region can be characterized by eddies (July 2014), by a sharp front (June 2009), or by a wide, gentle slope of isopycnals (September 1997) (Figures 2 and 3), and consequently has high standard deviations of properties (0.6°C and 0.06 salinity, Figure 4). In contrast, the upper ocean of the Hatton-Rockall Basin and the eastern Rockall Trough (around the European Slope Current) all have lower variability (standard deviation of $<$0.4°C and $<$0.004).

The mode waters are influenced by warm, saline Eastern North Atlantic Water of subtropical origin, the cooler, fresher Western North Atlantic Water of subpolar origin, and are modified by air-sea fluxes [*Brambilla et al*., 2008]. Isopycnal surfaces deepen from west to east as buoyancy is lost in the cyclonic horizontal circulation [*Lherminier et al*., 2007, 2010] and the downward slope is indicative of a net northward transport of the upper layer. All mode waters sampled by the EEL were shown by a Lagrangian study to be moving on average in a north-eastward direction [*Brambilla and Talley*, 2008].

The permanent thermocline (pycnocline) is consistently present at pressures of 900–1400 dbar in the Rockall Trough, and slopes upward to 400–900 dbar in the Iceland Basin (Figure 4). The sections in Figures 2 and 3 show that the thermocline is frequently shifted vertically from its mean position by mesoscale features, with the largest vertical movement observed in the Rockall Trough (e.g., compare the bowl-shaped thermocline in the western Rockall Trough in August 1985 with the domed thermocline in the same location in November 1989). This vertical movement of isopycnals contributes to the high standard deviation of properties associated with the mean fields (0.6°C and 0.04 in salinity, Figure 4). Cold, fresh, and stratified Sub-Arctic Intermediate Water (SAIW), saline Mediterranean Outflow water (MEDW), and in the Rockall Trough, Wyville-Thomson Overflow Water [*Johnson et al*., 2010], influence thermocline water properties.

The high stratification of the thermocline contrasts with the homogeneity of the underlying Labrador Sea Water, present as a deep layer of cool fresh intermediate water (3–4°C, 34.90–34.95), with low variability

(standard deviations of <0.2°C and <0.02 in salinity, Figure 4). The LSW is always fresher in the Iceland Basin than the Rockall Trough where it is present as a modified form. The properties of the LSW in both basins are the result of the original properties set during winter convection, as well as mixing with surrounding water types [*Yashayaev et al*., 2007a].

A layer of dense water is found in the Iceland Basin, where cold Iceland-Scotland Overflow Water (<3.0°C, Figure 4) forms a deep western boundary current. The ISOW is always more saline than the LSW that lies adjacent to it at 1000–2000 dbar in the northern Iceland Basin (Figures 2 and 3) and there is interleaving and mixing between the two water types. The mixing region is highlighted by higher standard deviations than the interior of LSW and ISOW (0.2–0.4°C and 0.002–0.004, Figure 4).

Having shown that there are regions of high variability observed by the EEL, we now examine the temporal variability by examining basin-mean vertical profiles (section 3.2) and layer-means of potential temperature and salinity (section 3.4).

3.2. Temporal Variability of Basin-Mean Vertical Profiles

In this section, we examine variability over the full depth water column. CTD profiles are separated into the three basins and averaged along isopycnals to create a mean potential temperature and salinity profile per basin per cruise. The profiles were reprojected on to pressure and Hovmöller plots were generated by interpolating to annual intervals (original spacing shown by tick marks on the time axis, Figure 6). Anomalies from the 1997–2014 mean are shown in Figure 7.

The vertical movement of isotherms and isohalines in the Hovmöller plots indicates changes in temperature and salinity from one cruise to another relative to constant pressure surfaces. Where contours deepen from left to right, the ocean has warmed and increased in salinity over time (shoaling contours indicate cooling and freshening). Figures 6 and 7 show that those changes are present over most depths and in all three basin, with time scales of 1–2 years (e.g., 0–1500 dbar from 1975 to 1980 in the Rockall Trough) to several years (e.g., a gradual shoaling of isotherms at 1000 dbar from 1997 to 2014 in the Hatton-Rockall Basin).

The vertical movement of the 27.20 kg m^{-3} isopycnal (base of the seasonally warmed surface layer) is indicative of the time of year of the cruise; the isopycnal is deepest during late summer/early autumn cruises (e.g., October 2006 and August 2007) and is absent in winter and spring cruises (e.g., May 2001 and May 1980).

In the upper ocean (27.20–27.50 kg m^{-3}), the temporal changes in the three basins are consistent with each other (Figure 7). From 1997 to 2001, there was an overall cooling and freshening, from 2001 to 2006 there was warming and increasing salinity, and from 2006 to 2014 there has been cooling and freshening.

There are earlier, persistent multiyear features evident in the longer Rockall Trough upper ocean time series. The 35.35 contour shows this most clearly; water of this salinity is absent from 1975 to 1980, present from 1980 to 1985, then absent for most of the upper ocean until 1995 when water >35.35 fills much of the upper ocean. Temperature does not always track the changes in salinity; the pattern described by the 35.35 contour is not so clear in potential temperature, instead water of >9.5°C is largely confined to the upper 300 dbar until 1995 when it begins the descent to 500 dbar, reaching that level in 2006.

The changes in the thermocline in the Iceland Basin follow the same pattern as the thermocline in the Rockall Trough (deepening of contours from 1997 to 2008 then shoaling to 2014), but the thermocline in the Hatton-Rockall Basin follows a different pattern, with gradual shoaling over the time series. In the anomalies (Figure 7), this is in evidence as long-term cooling and freshening in the shallow basin.

The intermediate waters (LSW, 27.70–27.85 kg m^{-3}) exhibit year to year changes and multiyear trends that sometime oppose the overlying water (Figure 7). In the Iceland Basin, the trend over the time series is for the contours to deepen, leading to warmer and more saline conditions, most notably in 2005–2010. In the Rockall Trough, the change over time is smaller but similar for the overlapping period; the 3.5°C contour gradually shoals over the course of the time series, while in salinity there is freshening from 1975 to 1995, followed by relatively stable salinity.

The changes over time in the whole water column include elements of heave (vertical movement of isopycnals) as well as water mass property changes. In the following sections, we explore water mass variability by

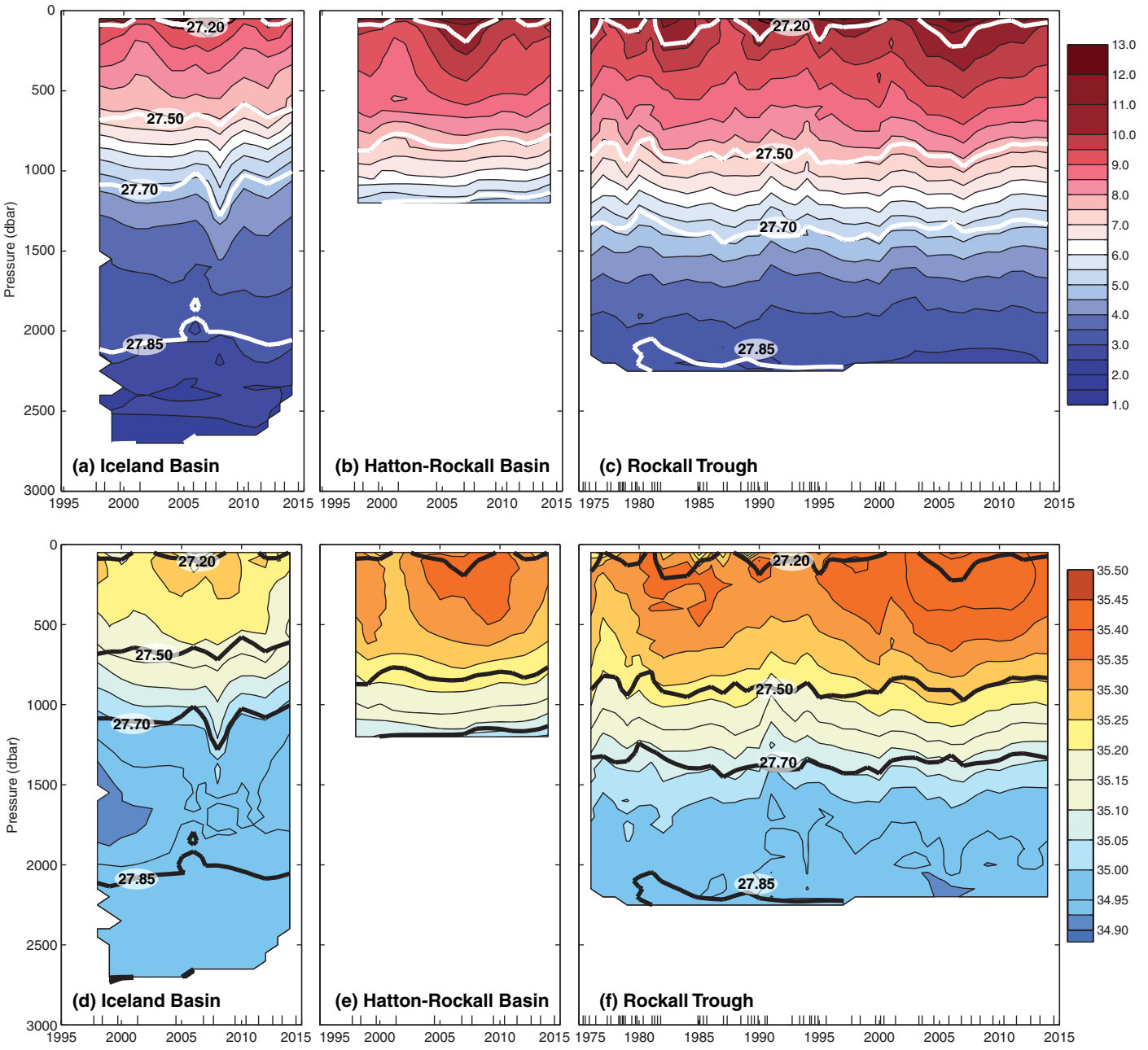

Figure 6. Temporal variability of section-mean vertical profiles (potential temperature °C on top row and salinity on bottom row). Mean profiles were created for the three basins from each cruise data set by averaging along isopycnals and reprojecting on to pressure. Profiles were interpolated to a regular time grid (annual spacing), with original cruise timing indicated by tick marks on the horizontal axis. Isopycnals used to define vertical layers in the text are highlighted as bold lines.

focussing on temporal changes in property means within density layers (Table 2). However, first we prove the robustness of the time series by investigating the associated uncertainties.

3.3. Layer-Mean Potential Temperature and Salinity: Uncertainty Estimates

In this section, we quantify uncertainty associated with the data in order to assess the representativeness and significance of the results. We consider two sources of uncertainty; data quality and irregular sampling. Some EEL cruises, mainly prior to 1991, have spikey CTD data (potential temperature and/or salinity) giving large scatter in the theta-S relationship (e.g., the data from 1990 in Figure 8; scatter at all depths indicates this is not only due to the presence of eddies). The method we use takes advantage of the way the thermocline water in the Rockall Trough is very well mixed, so that in high-quality data this part of the theta-S

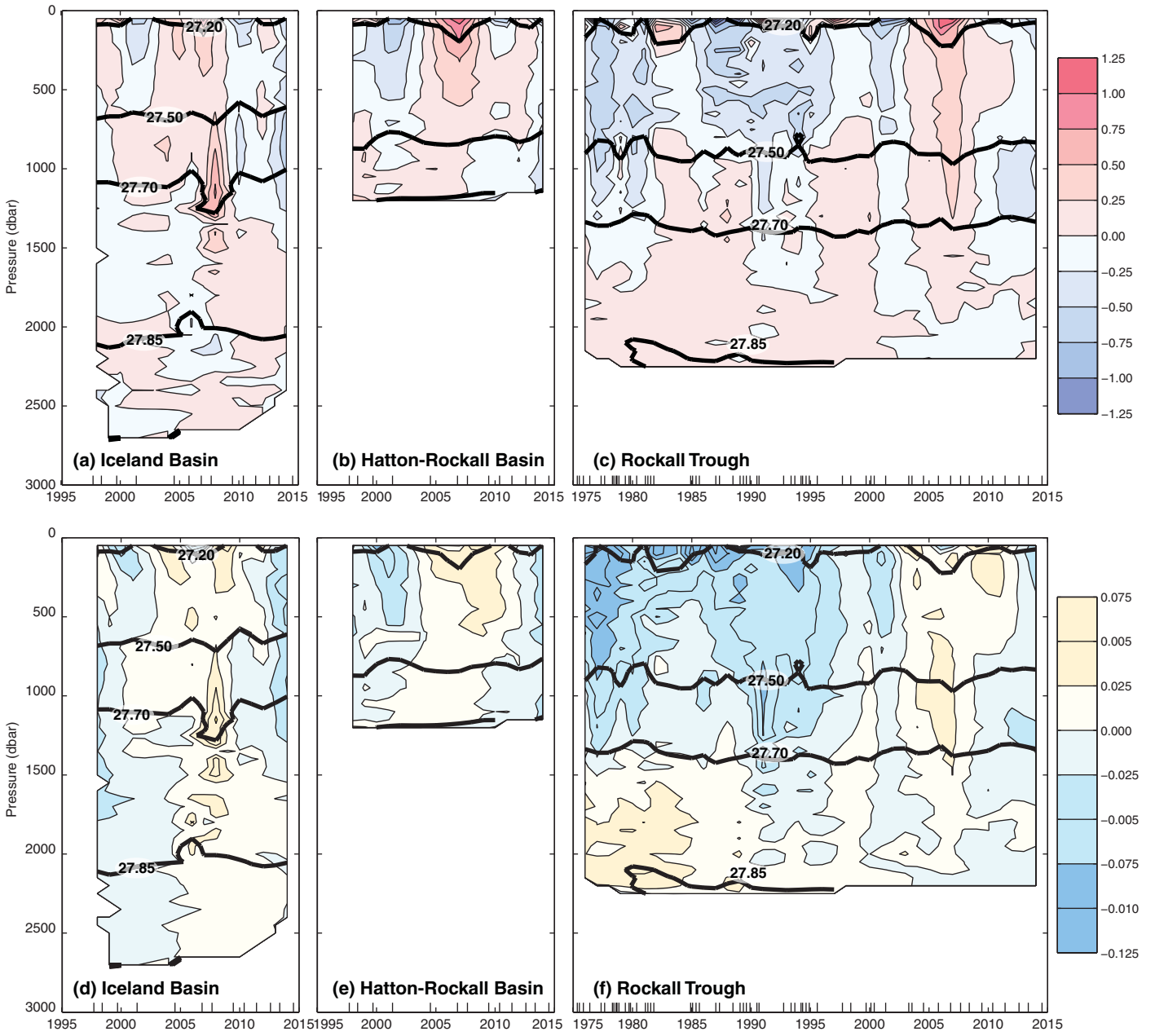

Figure 7. Temporal variability of section-mean vertical profiles (see Figure 6) as anomalies from 1997 to 2014 means (potential temperature anomaly °C on top row and salinity anomaly on bottom row).

curve is very tight (e.g., the data from 2010 shown in Figure 8). The scatter at density 27.60 kg m^{-3} is used to estimate the uncertainty; we define it as the standard deviation of properties at 27.60 kg m^{-3} for stations within the Rockall Trough. High-quality data (e.g., 2010 and 2011) give low values (order 0.01°C and 0.002 in salinity), while lower quality data give high uncertainty (e.g., 0.18°C and 0.030 in salinity for 1990) (Figure 8). This estimate does not include uncertainty due to accuracy of calibrations of potential temperature, salinity, or pressure (section 2.1).

A further source of uncertainty is aliasing of the time series due to irregular sampling, and especially the tendency since 1997 for annual cruises in the warmer months. The largest and most regular pattern of variability in the upper ocean is the annual cycle, and although our method ignores the seasonally warmed surface layer, the annual cycle will still influence the upper ocean results. High-frequency (subannual) variability will also be caused by mesoscale activity and response to local atmospheric conditions. Here we

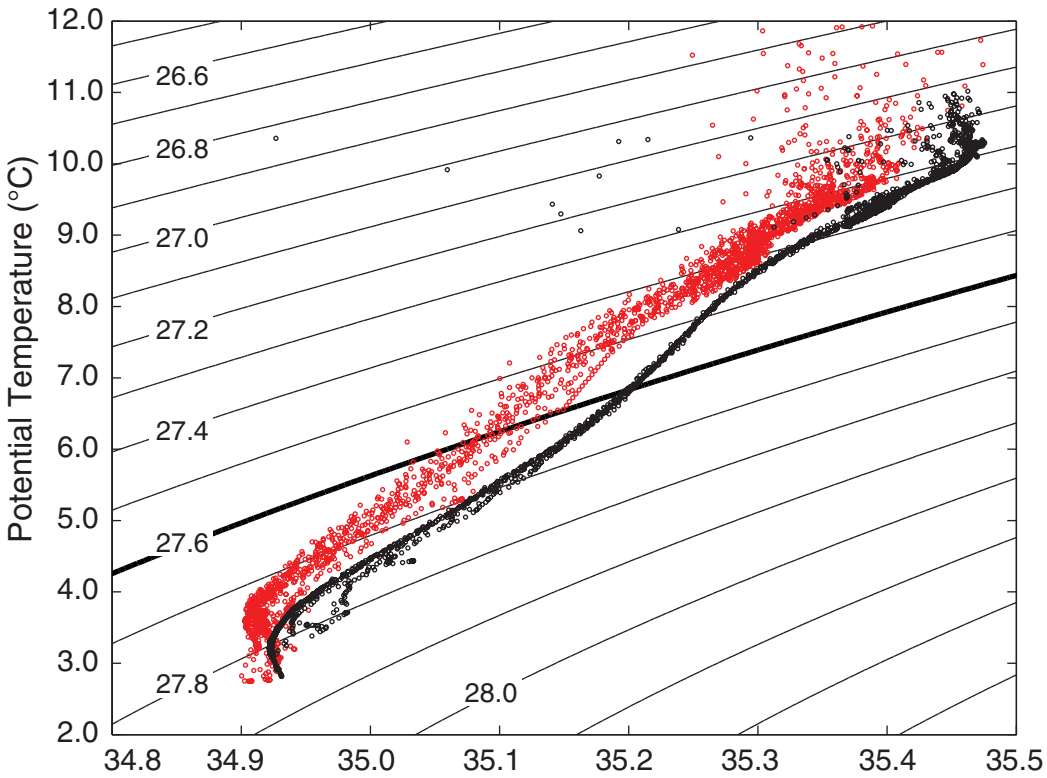

Figure 8. Potential temperature versus salinity from all deep Rockall Trough stations on Extended Ellett Line occupations in 2010 (black circles, illustrating good quality data with low scatter) and 1990 (red circles, illustrating poor-quality data with high scatter). The isopycnal at which the range of potential temperature and salinity are calculated during the error analysis (27.60 kg m^{-3}) is shown in bold.

establish the uncertainty ranges of the layer-means caused by the annual sampling strategy so that we can test the robustness of the means with respect to the aliasing.

We use the FLAME model output (section 2.2). The model was subsampled to create pseudosections in the location of the real hydrographic section, and divided into the three main topographic basins and vertical layers by density, as for the observations. We extracted time series, each at 3 day temporal resolution and 15 year duration, for the average temperature and salinity in each layer and each basin. As the hydrography of the model is comparable to the observations (not shown, see section 2.2), we use the variability in the model as an estimate for the variability in the real ocean.

Our uncertainty estimate is based on how close a data point at a single time step is to the corresponding annual mean over a window containing that data point. An estimate for the likely range for the difference between each point in the model time series and the mean is the standard deviation of the points in the time series in an annual window relative to the mean value over that annual window. Standard deviations over each annual, moving window along the 15 year model time series are computed and the mean of these standard deviations is reported as the uncertainty due to aliasing.

We have computed a set of time series of mean potential temperature and salinity for each density layer in each of the three main basins, with associated uncertainties (Figure 9). The uncertainty due to data quality is given by vertical error bars and the uncertainty due to sampling pattern is given by the thin lines forming envelopes around the time series. From 1975 to 1996, the uncertainty due to data quality varies considerably. In some cases, the uncertainty is high, but for many of the mean values, the error bars are small enough to suggest that there are significant differences between data points (though not often between data points collected within 1 year of each other). More recent cruises have lower data quality uncertainty, reflecting improvements in instrumentation and skill in data collection.

The uncertainty arising from the sampling strategy varies considerably by location and density layer. Lowest uncertainties are in the deepest layers; the LSW and the overflow water which are less influenced by

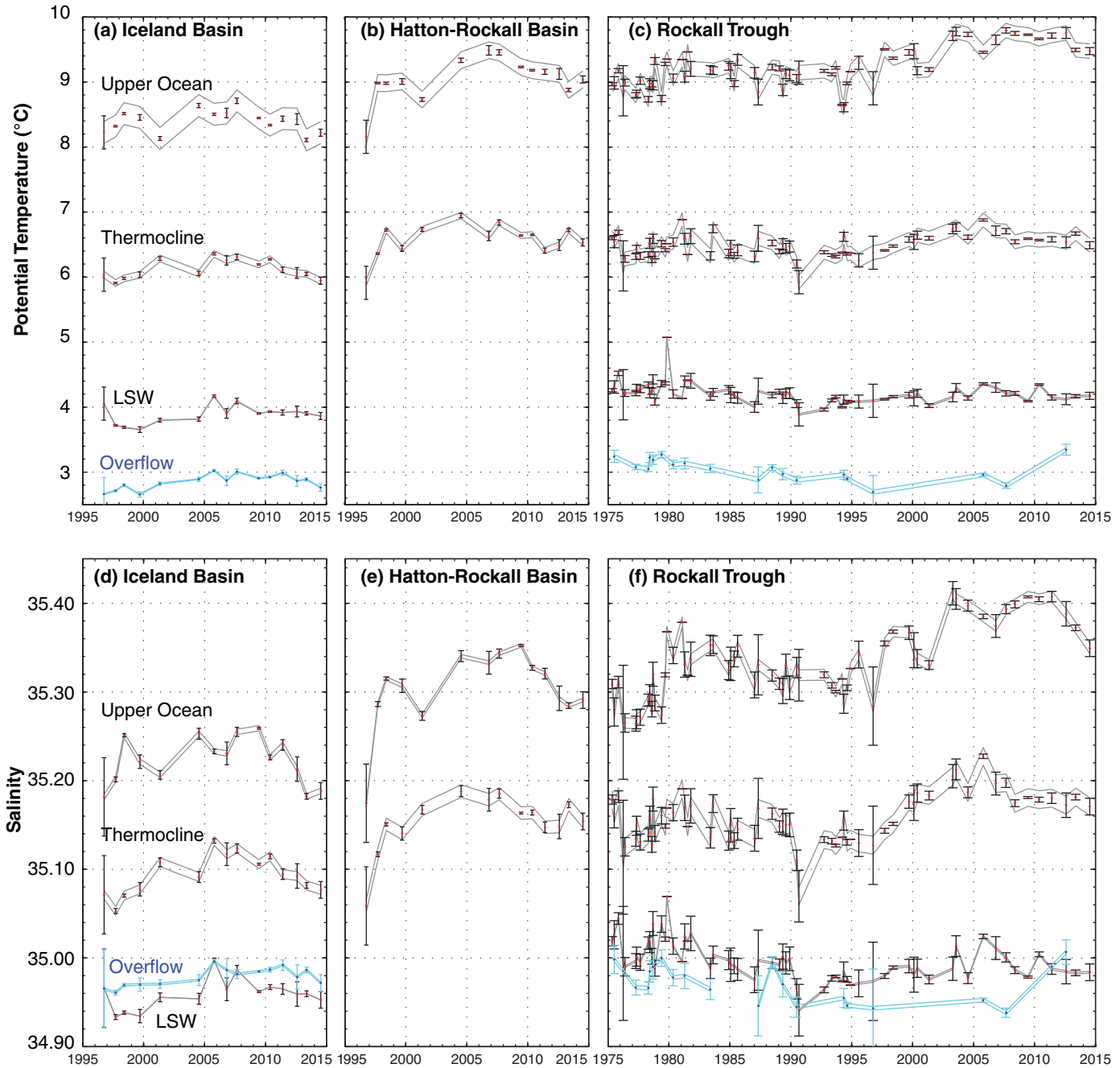

Figure 9. Time series of layer-mean potential temperature (top row) and salinity (bottom row) in the Iceland Basin (left column), Hatton-Rockall Basin (middle column), Rockall Trough (right column). The upper ocean is defined as potential density range 27.20–27.50 kg m^{-3} and excludes the seasonal mixed layer at the surface; the thermocline is potential density range 27.50–27.70 kg m^{-3}, Labrador Sea Water is potential density range 27.70–27.85 kg m^{-3}, and densest water (overflow) is greater than potential density 27.85 kg m^{-3} (shown in blue, not always present in Rockall Trough). Error bars represent uncertainty due to data quality. The bands given by thin lines are uncertainty arising through undersampling of intra-annual variability (not available for the densest layer).

seasonal cycles. As expected, some of the highest uncertainties in potential temperature are in the upper ocean where the seasonal cycle is large. Higher uncertainty is also present in regions of intense eddy activity, and the thermocline layer commonly has higher uncertainty in salinity than the upper layer.

The overall magnitude of the uncertainties compared to the variability leads us to conclude that EEL program is effectively detecting interannual to multidecadal variability in potential temperature and salinity between Iceland and Scotland.

3.4. Variability of Layer-Mean Potential Temperature and Salinity

With the robustness of the time series now established, we examine variability along the EEL. In the Rockall Trough, the length of the time series allows us to detect variability on timescales up to multidecadal. There are short periods of fresher conditions in the late 1970s as well as the late 1980s to early 1990s, and more saline conditions in the early 1980s with the highest values in the 2000s. Figure 9 confirms that potential temperature does not always covary with salinity; the fresher period in the late 1980s to early 1990s had potential temperatures largely unchanged from the preceding years. The amplitude of potential temperature and salinity changes are large ($\pm$0.6°C and $\pm$0.08 in salinity): at the peak conditions of the late 2000s, the mean was 1.2°C warmer and 0.15 more saline than the late 1970s. The magnitude of the variability is larger than that reported by *Holliday et al*. [2000] using data from 1975 to 1998 ($\pm$0.4°C and $\pm$0.05 in salinity). The upper ocean time series in the Hatton-Rockall Basin and Iceland Basin time series indicate that the properties change near concurrently across the region (within the temporal resolution of the data), though the magnitude is not identical between basins. Typically the changes are more exaggerated in the shallow Hatton-Rockall Basin and smallest in the Iceland Basin.

For most of the time series, and on decadal time scales the Rockall Trough thermocline displays the same pattern as the upper ocean (relatively saline in the 1980s, warmer and more saline 1997–2005). However in recent years (2008–2014), the properties of thermocline have exhibited different characteristics to the upper ocean, being quite stable while the upper ocean cools and freshens.

The Rockall Trough LSW time series shows a period of cooling and freshening from 1975 to the mid-1990s, followed by a lengthy period of slowly increasing potential temperature and salinity. The measurements in the Rockall Trough, although of a highly modified version of LSW, show a surprisingly similar pattern of change to the LSW in the Iceland Basin. The Iceland-Scotland Overflow Water exhibits a similar pattern of variability (not identical) which may well arise as a result of the mixing of the plume with the ambient en route from the sill to the location of the EEL. The dense water in the Rockall Trough is a different water type, and contains influence from Antarctic Bottom Water and Wyville-Thomson Overflow Water [*Johnson et al*., 2010]. Water of that density is frequently absent from the section, and although the series suggests variation similar to the LSW above, this cannot be stated with any certainty.

Having described the mean and variability in properties in the region, we next investigate the circulation by computing the mean and variability of velocity, transport, and overturning circulation.

4. Geostrophic Velocity, Transport, and Overturning Circulation

4.1. Method

Our goal in this analysis is to quantify the time-mean integral of the volume flux in different water masses across the EEL. Hence we determine a reference level on broad horizontal scales and over a long-term mean, being less concerned with the details of individual eddies or the correlations of velocities and properties at the mesoscale (similar approach to *Gourcuff et al*. [2011]). Our method is a combination of matching each cruise to the mean basin-scale circulation from Aviso absolute sea-surface height slope, with a heuristic adjustment for the eastern Iceland Basin.

Geostrophic velocities were computed between pairs of CTD stations using the CSIRO SEAWATER routines (V1.2d). Geopotential anomalies were calculated relative to the sea surface from potential temperature, salinity and pressure data and from these we computed geostrophic velocities. In the bottom triangle, (water below the deepest common level of each station pair) we assume a constant velocity equal to the that at the deepest common level. To calculate absolute geostrophic velocities and transports, an assumption about a level of no motion (LoNM), or level of known motion, must be made. The sloping nature of the thermocline means that isopycnals are more suitable than pressure surfaces for a LoNM, and the optimum surface may be different in each basin. The thermocline deepens west to east across the Iceland Basin from around 500 m to 800 m, whilst in the Rockall Trough it is found at around 1000 m (Figures 2–4). This is caused by separate sources of water to the two basins; in the Iceland Basin we see cooler and fresher Western North Atlantic Water (NAW) carried in the North Atlantic Current, whilst the Rockall Trough contains Eastern NAW which has travelled northwards from the intergyre area near the Bay of Biscay [*Holliday et al*., 2000; *Johnson et al*., 2013].

To determine the optimum LoNM, we compare the Aviso absolute sea-surface height slope with the geopotential sea-surface slope on a basin wide scale: the geopotential sea-surface heights are computed relative to each isopycnal in turn. The isopycnal which minimizes the difference in slopes is defined as the LoNM. Because we impose a zero velocity reference at the LoNM, then this is the isopycnal on which there would be a minimum adjustment to the circulation to match the two surface circulations. For each EEL, occupation geopotential height was computed relative to potential density levels ranging from σ_0=27.40 kg m^{-3} to σ_0=27.80 kg m^{-3} in steps of 0.02 kg m^{-3}. The Aviso absolute sea surface heights were interpolated on to the station positions from a daily data file on the central date of each cruise. The standard deviation of the differences between the altimeter sea surface heights, and sea surface geopotential heights, were computed for each cruise and basin. Comparing these standard deviations against the isopycnal potential densities for the Iceland Basin and Rockall Trough separately, determines which isopycnal produces the minimum difference in sea-surface slope across both basins during each individual cruise. The range in the optimum potential density for all cruises was small ($\pm$0.03 kg m^{-3} and $\pm$0.02 kg m^{-3} for the Iceland Basin and Rockall Trough, respectively). Consequently we select an initial LoNM for of 27.57 kg m^{-3} for the northern and central Iceland Basin, and 27.68 kg m^{-3} for the Rockall Trough.

We further modify the LoNM heuristically as follows. In the northern and western Iceland Basin, a midwater column LoNM seems reasonable due to the upper waters flowing north-eastward and the underlying LSW and ISOW flowing toward the south-west. Similarly in the central Iceland Basin as water denser than 27.80 kg m^{-3} is known to flow south-westward [*Kanzow and Zenk*, 2014] a mid depth flow reversal is again expected. Further east in the Rockall Trough, the upper waters are known to move in a northward direction in the west of the basin and a southward direction to the east—excluding the northward flowing European Slope Current over the shelf [*Ellett and Martin*, 1973; *Holliday et al*., 2000]. As the underlying LSW recirculates cyclonically [*Holliday et al*., 2000], with any overflow water flowing southward in the western trough [*Johnson et al*., 2010], using a mid depth LoNM again seems justified. Indeed this has been observed with moored current meters along the EEL in the Rockall Trough [*Holliday et al*., 2000]. However, in the eastern Iceland Basin the upper waters, LSW and ISOW are all moving in a general north-eastward direction; the recirculation of ISOW in this area being confirmed by current meter measurements [*Kanzow and Zenk*, 2014]. Therefore in the eastern Iceland Basin, and shallow Hatton-Rockall Basin, no flow reversal is expected mid water column and we consider the LoNM to be at the seabed. Further, at particular stations where the largest observed density is less than the LoNM we assume zero velocity at the seabed.

The total error introduced by using a time-constant LoNM was estimated by calculating transports using both the lower and upper bound of the LoNM for each basin (i.e., 27.54–27.60 kg m^{-3} in the Iceland Basin, and 27.66–27.70 kg m^{-3} for the Rockall Trough). This gave errors for total transport across the two basins of $\pm$0.5 Sv and $\pm$0.2 Sv, respectively. It is probable that a comparison of Aviso and geopotential heights at higher horizontal resolution would identify a significant velocity on the reference isopycnal in the eastern Iceland Basin. Our method does constrain our solutions to the basin-scale mean circulation that is part of the Aviso mean dynamic topography. However, at small scales and particularly at the boundaries, and for a number of strong mid-ocean jets, our solutions have higher horizontal resolution through the observed density field than would be obtained by constraining the solutions to the Aviso data on a station-by-station basis.

4.2. Mean and Variability of Geostrophic Velocity

Upper water movement in the Iceland Basin is predominantly north-eastward (Figure 10) with flow concentrated in three currents: in the western Iceland Basin (30 km), central Iceland Basin (360 km), and eastern Iceland Basin (520 km). A fourth branch is observed in the western Hatton-Rockall Basin at 600 km. There is some evidence of upper water recirculation in the Iceland Basin at 180 km as evidenced by slightly more saline waters (35.23–35.25) and small south-westward velocities of up to $-$0.02 m s^{-1}. In the Rockall Trough, the well-documented anticyclonic recirculation around the Anton Dohrn seamount (980 km) is clearly seen, with velocities reaching 0.06–0.08 m s^{-1}. In the far east of the EEL, a strong northward flow (0.08–0.10 m s^{-1}) is observed over the continental slope with the fastest velocities being associated with the most saline water (>35.43) carried in the European Slope Current.

In the Iceland Basin, the LSW (27.70–27.85 kg m^{-3}) is associated with relatively low velocities ($\pm$0.02 m s^{-1}); however, in the Rockall Trough, a cyclonic circulation is seen (Figure 10b). Flow is northwards east of the Anton Dohrn seamount (0.04–0.06 m s^{-1}) with southward flow to the west ($-$0.02 to $-$0.04 m s^{-1}).

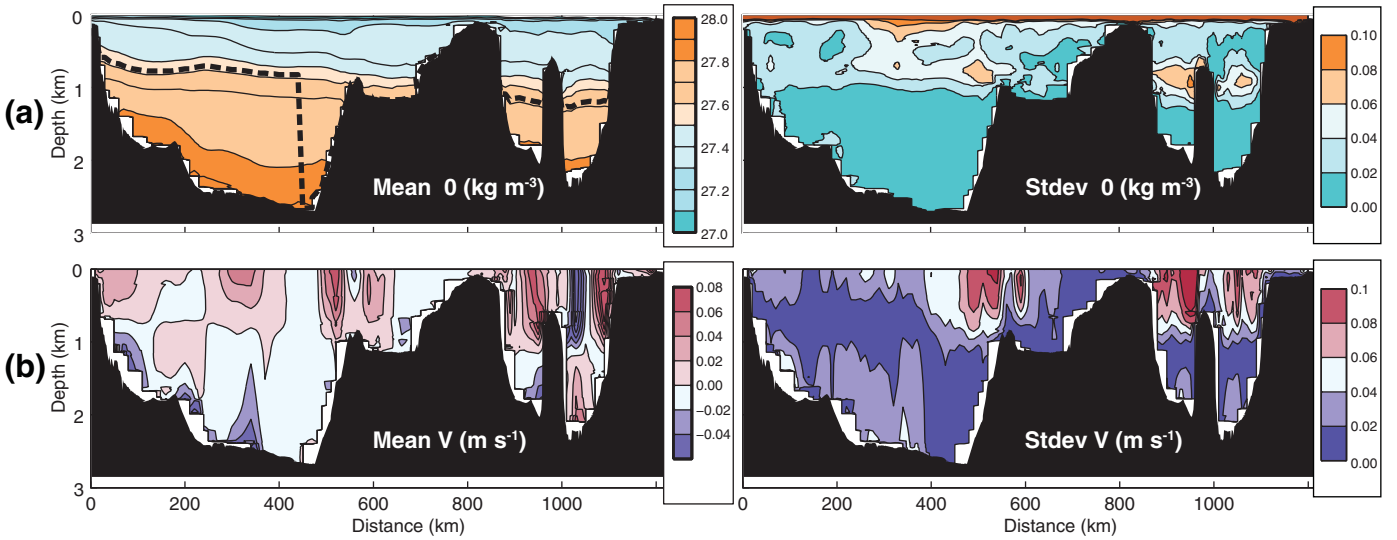

Figure 10. Mean sections across the Extended Ellett Line and associated standard deviations for (a) potential density (kg m^{-3}, as shown in Figure 4), and (b) geostrophic velocities (m s^{-1}). Fields calculated from 11 complete occupations between 1997 and 2014 (Table 1). Dashed black line in Figure 10a (left) shows the level of no motion used in geostrophic calculations. In Figure 10b (left) positive values indicate flow toward the Nordic Seas.

Two components of overflow water are known to influence the EEL. In the Iceland Basin, ISOW which enters through the Faroe Bank Channel is a saline water mass which hugs the Icelandic Slope and Reykjanes Ridge, and is clearly associated with westward/south-westward flow between 0 and 400 km. The much smaller presence of Wyville Thomson Ridge Overflow Water in the Rockall Trough is observed as lifting of isohalines between 1200 m and the seabed along the eastern flank of Rockall Bank (860–880 km).

Past studies have indicated that the Iceland Basin and Rockall Trough have regions of high mesoscale activity related to the major current paths [e.g., *Heywood et al.*, 1994; *Hakkinen and Rhines*, 2009]. Similarly in our observations, higher variability in salinity coincides with the position of the north-eastward currents in the central Iceland Basin (360 km), eastern Iceland Basin (520 km), and on the west of the Hatton-Rockall Basin (600 km) (Figure 4). There is no increased variability in salinity linked to the branch at 30 km in the Iceland Basin, or the small recirculation feature at 180 km. Similarly, in the Rockall Trough, there is no increased salinity variability associated with the southward flowing upper water (1020 km) or northward flowing European Slope Current in the east of the basin (1080 km). A weaker signal of higher variability is seen, however, in the northward flowing upper water in the western trough (920 km).

The largest standard deviations in geostrophic velocity are associated with some of the northward flowing upper water currents, as well as the deep southward flowing ISOW. Interestingly the largest variabilities (>0.08 m s^{-1}) are observed in the eastern currents: those in the eastern Iceland Basin (520 km), the western Hatton-Rockall Basin (600 km), the western Rockall Trough (920 km), and over the European Slope (1080 km). Increased variability is also associated with the southward flowing upper water in the Rockall Trough at 1020 km. However, the two currents in the northern and central Iceland Basin (30 km and 360 km, respectively) have only smaller variability (0.02–0.04 m s^{-1}) associated with them.

4.3. Zonally Integrated Volume Transports

The mean net transport of upper waters (27.20–27.50 kg m^{-3}) across the entire EEL is 6.7 ± 3.7 Sv, with 3.9 ± 1.9 Sv transported in the Iceland Basin, 2.3 ± 1.3 Sv in the Rockall Trough and only 0.5 ± 0.5 Sv in the Hatton-Rockall Basin (Table 3 and Fig 10b). The three north-eastward currents in the Iceland Basin (at 30, 360, and 520 km) are associated with transports of 0.7 ± 0.3 Sv, 1.3 ± 0.6 Sv, and 1.0 ± 0.4 Sv, respectively, while the small recirculation at 180 km has a transport of −0.1 ± 0.1 Sv. A north-eastward flow of 0.9 ± 0.3 Sv is situated on the eastern slope of Hatton Bank at 600 km; while the two northward currents in the Rockall Trough, centered on 920 km and 1080 km, have transports of 1.9 ± 1.3 Sv and 1.8 ± 0.4 Sv, respectively. Whereas any recirculation in the Iceland Basin is small (total −0.5 ± 0.4 Sv); the Rockall Trough shows a clear recirculation around the Anton Dohrn seamount. West of this feature 1.9 ± 1.3 Sv of upper waters flow

Table 3. Mean Geostrophic Transports ± One Standard Deviation (Sv) for Different Portions of the EEL and Various Water Masses[a]

	Iceland Basin	Hatton-Rockall Basin	Rockall Trough	Entire EEL
Total transport (Sv)	−2.0 ± 4.5	0.6 ± 0.4	2.8 ± 0.8	1.4 ± 5.8
Upper water transport (Sv)	3.9 ± 1.9	0.5 ± 0.5	2.3 ± 1.3	6.7 ± 3.7
Thermocline transport (Sv)	−0.1 ± 0.7	0.0 ± 0.0	0.1 ± 0.0	0.1 ± 0.8
LSW transport (Sv)	−3.8 ± 2.4[b]	0.0 ± 0.0	−0.2 ± 0.1	−4.0 ± 2.4
OW transport (Sv)	−2.1 ± 0.9	0.0 ± 0.0	0.0 ± 0.0	−2.1 ± 0.8

[a]Values were calculated from 11 complete occupations between 1997 and 2014 (Table 1). Positive transports indicate flow toward the Nordic Seas, and negative ones flow away from the Nordic Seas. Layer definitions are given in Table 2.
[b]There is significant mixing between LSW and OW in the north Iceland Basin and some of the southward flow in the LSW category is an admixture of these two water masses; see text for more information.

northward, while to the east a southward flow of −1.4 ± 0.2 Sv is observed. Transport within the thermocline waters (27.50–27.70 kg m^{-3}) is small with a mean transport of 0.1 ± 0.8 Sv across the entire EEL section (Table 3 and Figure 11c).

The net transport of waters with densities between 27.70 and 27.85 kg m^{-3} between Iceland and Scotland is −4.0 ± 2.4 Sv (Table 3) with ∼70% of this transport being in the first 400 km of the section and 95% within the Iceland Basin (Figure 11d). Transport across the Hatton-Rockall Basin is 0.0 Sv due to the shallow nature of the plateau. Circulation of LSW in the Rockall Trough is cyclonic with −0.6 ± 0.0 Sv flowing southward in the west of the basin, and 0.7 ± 0.1 Sv northward in the east. The transport of the densest class of water (>27.85 kg m^{-3}), which consists predominantly of ISOW, is confined to the northern and central Iceland Basin with a net transport of −2.1 ± 0.9 Sv in this area (Table 3 and Figure 11e). No flow is observed in the Rockall Trough due to the lack of sufficiently dense water.

4.4. Overturning Stream Function

The overturning stream function is an integral quantity of the circulation that can be discussed in terms of thermohaline forcing of the Atlantic. Here two stream functions are defined in depth (ψ(z)) and density space ($\psi(\rho)$). Equation (1) is defined in a coordinate system that follows on naturally from the calculations of geostrophic velocity. However, when there may be north-south recirculation at the same density, and isopycnals are sloping such as along the EEL, diabatic processes of water mass transformation may be incorrectly inferred from equation (1). This effect has been discussed extensively for the Southern Ocean's Deacon Cell [*Döös and Webb*, 1994; *Kuhlbrodt et al.*, 2007]. As such, the overturning stream function is computed both in pressure (equation (1)) and density space (substitute ρ for z in equation (1)).

$$\Psi(z) = \int_0^z \int_{x_{west}}^{x_{east}} v(x', z')\, dx'\, dy' \tag{1}$$

A similar analysis for hydrographic sections between Greenland and Portugal found that if pressure coordinates were used, slight changes in the distribution of horizontal flows over sloping bathymetry lead to significant variability in the overturning stream function [*Lherminier et al.*, 2007]. In contrast, when the stream function was computed in density coordinates, it was much less sensitive to such circulation constraints. For the EEL section, the stream function maxima in both pressure and density coordinates are nearly identical (Table 4 and Figure 12). Thus for this eastern portion of the subpolar gyre, there is little sensitivity to depth or density as the vertical coordinate system when defining the time-mean stream function. In the Rockall Trough, the mean maximum northward flow is 3.0 ± 3.7 Sv at 1145 m and 27.65 kg m^{-3}; using density coordinates a small net southward flux is seen at densities >27.75 kg m^{-3}. The mean maximum northward flow in the Iceland Basin (4.4 ± 2.0 Sv) is at a shallower depth and lower mean density (815 m and 27.57 kg m^{-3}) than in the Rockall Trough. Variability in the maximum stream function is larger in the Rockall Trough than in the Iceland Basin. Therefore, although the Iceland Basin has the larger transport, it is the Rockall Trough that dominates the net variability in the overturning along the EEL.

5. Summary and Discussion

The subpolar waters measured by the EEL eventually flow into the Arctic Ocean as Atlantic Water, or are exported southward from the subpolar gyre as North Atlantic Deep Water. As a result, changes in the

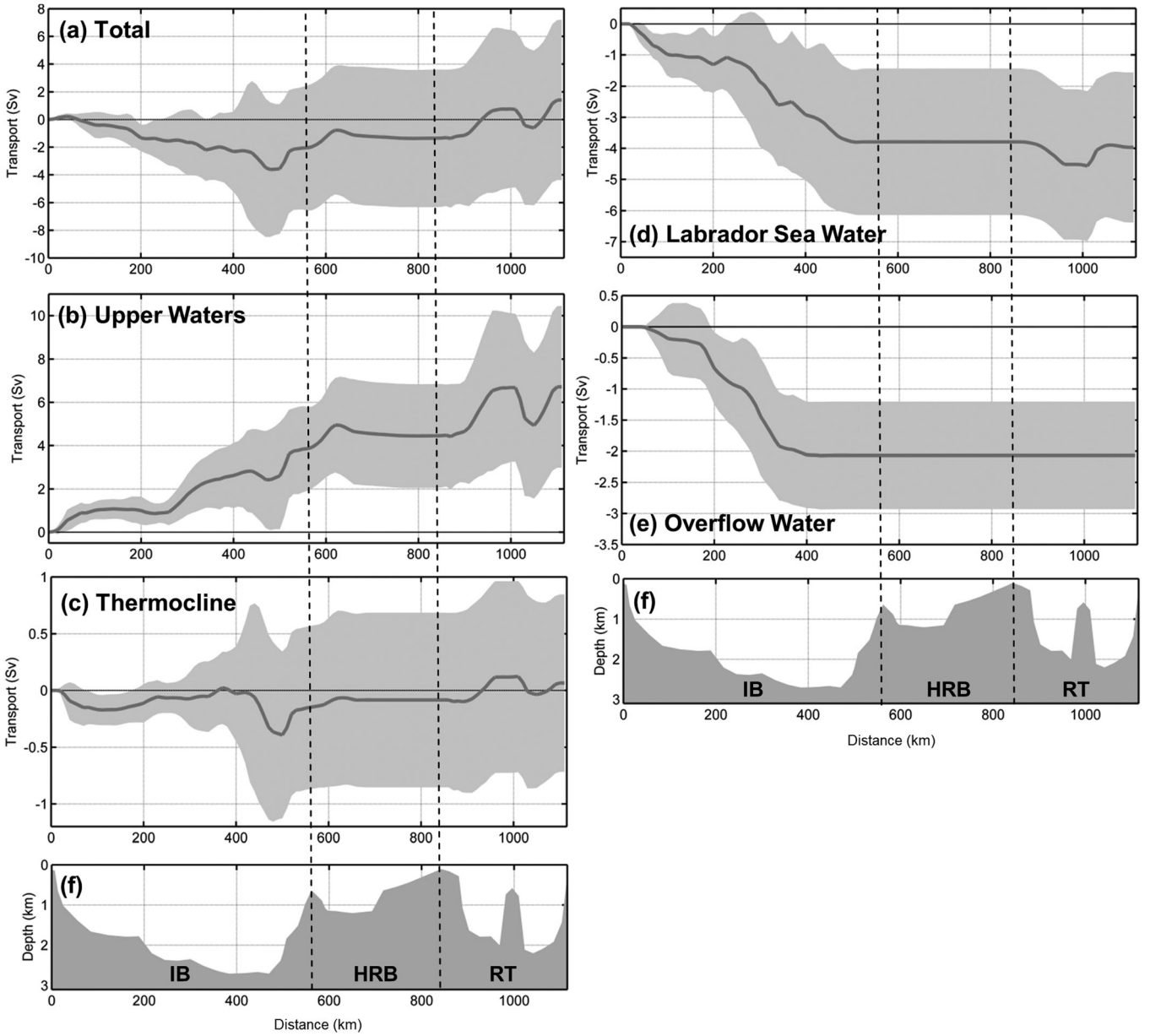

Figure 11. Zonally cumulated geostrophic transport (Sv) across the Extended Ellett Line for (a) the entire water column, (b) upper waters, (c) thermocline waters, (d) Labrador Sea Water, and (e) overflow waters. Please note different *y*-axes. Gray lines show the mean and gray shading ± one standard deviation. Transports were calculated from 11 complete occupations between 1997 and 2014 (Table 1). Positive values indicate flow toward the Nordic Seas. Water mass definitions are given in Figure 5. Figure 11f show bathymetry with: IB – Iceland Basin; HRB – Hatton-Rockall Basin; and RT – Rockall Trough.

potential temperature and salinity in the eastern subpolar gyre propagate to the highest latitudes and to the deep limb of the overturning circulation. In this study, we have analyzed 4 decades of hydrographic observations to describe the interannual to multidecadal changes in potential temperature, salinity, velocity,

Table 4. Maximum Mean Overturning Streamfunction ± One Standard Deviation (Sv) for Different Portions of the EEL Accumulated on Pressure Surfaces—$\psi(z)$ and Isopycnal Surfaces—$\psi(\rho)$[a]

	Iceland Basin	Rockall Trough	Entire EEL
$\psi(z)$ (Sv)	4.3 ± 1.9 (815 m)	3.0 ± 3.7 (1145 m)	7.8 ± 4.3 (925 m)
$\psi(\rho)$ (Sv)	4.4 ± 2.0 (27.57 kg m^{-3})	3.0 ± 3.7 (27.65 kg m^{-3})	8.1 ± 4.4 (27.62 kg m^{-3})

[a]Positive transports indicate flow toward the Nordic Seas.

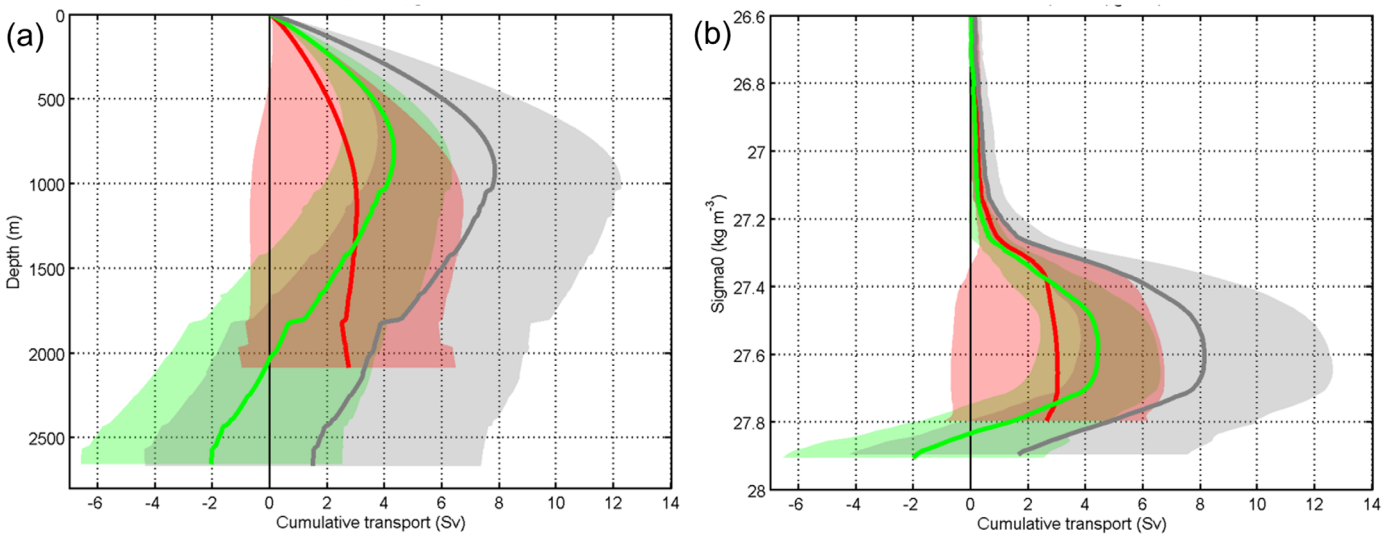

Figure 12. Overturning stream function (Sv) for various parts of the Extended Ellett Line calculated in (a) pressure coordinates (m) and (b) density co-ordinates (kg m^{-3}). Colored lines show the mean, and shading ± one standard deviation. Gray entire Extended Ellett Line; green: Iceland Basin; and red: Rockall Trough. Values were calculated from 11 complete occupations between 1997 and 2014 (Table 1). Positive transports show flow toward the Nordic Seas.

and transport of the shallow, intermediate, and deep ocean. We have shown through quantifying uncertainty arising from data quality issues as well as the sampling rate, that a robust pattern of interannual to multidecadal variability is revealed by the time series. We have presented two previously unpublished time series that characterize two decades of changes in the properties of the deep ocean Iceland and Hatton-Rockall Basins, and provided an update of a longer time series in the Rockall Trough. We have presented a new view of the mean velocity field and transport across the section and computed that the maximum overturning circulation is close to 8 Sv in this part of the subpolar region.

The variability of temperature and salinity is highest in the NAC region of the upper ocean, the Rockall Trough thermocline, and the region of mixing between ISOW and LSW in the Iceland Basin. Property variability is lowest in the main body of LSW in the Iceland Basin, the Hatton Rockall Basin, and in the European slope current. Velocity variability is greatest in the Rockall Trough upper ocean, which means that this is where the largest variability in overturning circulation is located. Interestingly the northward current situated over the Scottish Shelf (which is at least partly composed of the European Slope Current) is less variable than the rest of the basin in terms of both velocities and transports. Velocity is also highly variable in the NAC zone of the Iceland Basin, and the associated high standard deviation of properties implies that the NAC region may have the largest variability in heat and freshwater transport. The international OSNAP project (Overturning in the Subpolar North Atlantic Program) is making direct and continuous measurements of the overturning circulation of the whole subpolar North Atlantic from 2014 to 2018 and will quantify variability on seasonal to interannual time scales. The program will investigate how and why the eastern basin dominates variability. Future analysis will draw in observations from the EEL and OSNAP to examine how properties and transport covary, and to investigate the long-term variability of heat and freshwater transport in the eastern subpolar region.

Temperature and salinity vary on interannual to decadal time scales at all depths. The upper ocean has notably saline periods in 1980–1986 and after 1995. Since 1997, all three basins vary in the same way, with a minor cooling and freshening from 1997 to 2001, warmer and more saline from 2001 to 2006, and cooler and fresher from 2006 to 2014. The large overall increase in temperature and salinity observed since 1997 means that the amplitude of variability of the full 1975–2014 time series (±0.6°C and ±0.08 in salinity) is greater than that reported by *Holliday et al*. [2000] using data from 1975 to 1998 (as ±0.4°C and ±0.05 in salinity). On decadal time scales the property changes observed by the EEL are consistent with those observed in the Nordic Seas and in the central subpolar gyre regions like the western Iceland Basin and the central Labrador Sea [e.g., *Beszczynska-Möller and Dye*, 2013]. That level of consistency over very large areas implies that the upper ocean has strong advective memory; in other words, that anomalies, once

established in a ventilated region, can persist for many years as they are transported around and through the region.

In the Rockall Trough, temperature does not always follow the same pattern as salinity; only slight warming is in evidence as salinity increased from 1980 to 1985, and after 1986 as salinity declined, the temperature remained stable. Since 1995, the overall increase in salinity in the Rockall is accompanied by increasing temperature. Different mechanisms led to the freshening during the 1970s and the increased salinity of the 1990s and 2000s. The very low salinity in the 1970s (the Great Salinity Anomaly) [*Dickson et al*., 1988] was caused by a major influx of Arctic freshwater in the form of sea-ice exported through the Fram Strait. The event was first observed northwest of Iceland and propagated through the subpolar gyre and the Nordic Seas over the course of about 10 years, reaching the Rockall Trough after about 7 years. In most regions of the subpolar North Atlantic and the Nordic Seas, the GSA was accompanied by low upper ocean temperatures but this is less clear in the Rockall Trough. In contrast, the dramatic rise in salinity after the mid-1990s is actually first seen in the Rockall Trough and Iceland Basin and propagates into the Nordic Seas and central subpolar gyre over the following 5 years. The feature is understood to be the manifestation of increased transport of southern origin water masses (see below) and is accompanied by a corresponding rise in temperature in all open ocean subpolar and Nordic regions. Likewise, the indication of a freshening since 2010–2011 in the EEL basins is also accompanied by cooling. This intriguing distinction between the thermal response in the Rockall Trough upper ocean to pulses of low or high salinity with either a northern or southern source is yet to be properly understood; we speculate that air-sea heat flux dampened the cooling in the 1970s and may have enhanced the warming since 1995. This is a topic for further investigation.

Recent research has established that the cause of the overall increase in potential temperature and salinity of the upper ocean from the late 1990s to the mid-2000s was a change in the circulation of the subpolar gyre and the inflow of subtropical waters. The subpolar gyre circulation decreased, and at the same time, the subpolar front moved westward and more subtropical water entered the eastern region [*Holliday*, 2003]. The Hatton-Rockall Basin lies within the region where the subpolar front shifts either northwestward or southeastward which is the likely reason why property extremes are highest there. The mechanisms driving the changes are still being examined, with contributing effects from the NAO, wind stress curl, blocking highs, and transport of anomalies from the subtropics all being proposed [*Hakkinen and Rhines*, 2004; *Hátún et al*., 2005; *Hakkinen et al*., 2011a, 2011b; *Desbruyeres et al*., 2013]. The observations presented here are consistent with the present understanding of the basin-scale circulation changes to 2010 [*Hughes et al*., 2012]. The decrease in potential temperature and salinity after 2010 in all basins provides the first new evidence that the eastern subpolar North Atlantic is once again being influenced by cold, fresh western subpolar water. Whether this implies a sustained expansion of the subpolar gyre into the region remains to be seen.

Observations of layer-mean temperature and salinity reveal that in the Rockall Trough the upper ocean covaries with the thermocline on decadal time scales. We have also seen that on time scales of less than 5 years, the two layers can behave differently. The thermocline waters are heavily influenced by SAIW subducted at the NAC and the MEDW. The influence of MEDW has been shown to extend further north and westward when the subpolar gyre is in a contracted state, meaning that the thermocline not only has less cool, fresh influence, it also has more warm, saline influence [*Lozier and Stewart*, 2008; *Stentardo et al*., 2015]. The SAIW has less influence in the eastern subpolar gyre when the polar front is situated further west, so our observations that the thermocline property changes reflect that of the upper ocean on decadal scales are largely consistent with understanding of the subpolar gyre. However, there are as yet unexplained differences in the variability between the thermocline waters and the upper ocean; this is a topic for ongoing research.

The LSW in the Rockall Trough shows freshening and cooling from 1975 to 1995, followed by a period of warming and increasing salinity. Since 1997 the LSW in the Iceland Basin follows the same pattern as the Rockall Trough, despite having different mean properties resulting from significant mixing en route from the Labrador Sea to the eastern basins [*Yashayaev et al*., 2007b]. The implication of the similarity is that the forcing that creates the variability applies consistently to both basins.

We have computed mean and variability of geostrophic velocity and transport. The level of no motion for geostrophic calculations was determined heuristically and by numerical comparison with AVISO absolute sea-surface heights, and is entirely consistent with literature and observations. Between Iceland and

Scotland, the net upper water transport (6.7 ± 3.7 Sv) is in a north/north-eastward direction toward the Nordic Seas. Flow is concentrated in six currents: three in the Iceland Basin (total 3.9 ± 1.9 Sv), one in the eastern Hatton-Rockall Basin (0.9 ± 0.3 Sv), and two in the Rockall Trough (total 3.7 ± 1.7 Sv). Although the largest transports are seen in the Rockall Trough currents (1.9 ± 1.3 Sv and 1.8 ± 0.4 Sv), net transport through the basin is only 2.3 ± 1.3 Sv due to a large southward recirculation to the east of the Anton Dohrn seamount.

These values agree well with previous estimates. Net upper water flow through the Iceland Basin derived from multiple ship-borne ADCP transects was 4.8 Sv; while flow in the Rockall Trough was 3.5 Sv [*Chafik et al*., 2014] and flow between Iceland and Scotland 6.1 ± 0.3 Sv [*Childers et al*., 2014]. Previous geostrophic calculations have determined net upper water transports of 2.7–3.7 Sv for the Rockall Trough [*Ellett and Martin*, 1973; *Holliday et al*., 2000] and 7.6 ± 0.9 Sv between the Reykjanes Ridge and Scotland [*Sarafanov et al*., 2012]. Around 60% of the upper water transport between Iceland and Scotland passes through the Iceland Basin, ∼5% through the Hatton-Rockall Basin and ∼35% through the Rockall Trough. Since only ∼ 50% of the estimated 7 Sv inflow between Iceland and Scotland crosses the Greenland-Scotland Ridge between Iceland and the Faroes [*Østerhus et al*., 2001], some 10% of the flow must cross from the Iceland Basin into the very northernmost Rockall Trough prior to entering the Nordic Seas.

The mean velocity and transport fields (Figure 10) shows almost entirely eastward velocity in the upper layer of the Iceland Basin, which is slightly different to our expectations of some westward flow at the northern end of the section [e.g., *Brambilla and Talley*, 2008]. The variability (expressed as standard deviation of the mean, see Table 3) includes westward flow in some individual sections, but the uncertainty associated with transports computed from individual sections is very high. It is possible that our mean estimate excludes some westward barotropic flow due to the methodology, and it is also possible that westward return flow takes place west of the section when the subpolar gyre is in a contracted state (which is the case for much of this time series). These issues are currently being investigated by analyzing satellite altimetry data and lowered ADCP data.

The ISOW flux in the Iceland Basin (−2.1 ± 0.9 Sv) again agrees well with previous transport estimates from a variety of sources (1.2–5.4 Sv, mean 2.5 Sv) summarized in *Kanzow and Zenk* [2014]. There is agreement despite the slightly denser upper bound definition (27.85 kg m^{-3} versus 27.80 kg m^{-3}). A small southward flow is observed below 27.70 kg m^{-3} in the overturning stream function computed in density coordinates (−0.3 ± 0.3 Sv, Figure 12). As this flow is in the density range of Wyville Thomson Ridge Overflow Water, and in the expected location (western Rockall Trough, Figure 11d), it raises the interesting possibility of whether this southward flow can be attributed to the water mass. However, the magnitude of the flow is very variable and close to errors expected with the analysis.

One would expect the net LSW flux in the Iceland Basin to be around 0 Sv, as is true in the Rockall Trough. Like the Rockall Trough, the Iceland Basin has no connections deeper than 1200 m except in the south, suggesting that LSW must both enter and leave the basin via this southern entrance [*Ellett et al*., 1986; *Holliday et al*., 2000]. The large net southward flow (−3.8 ± 2.4 Sv) in this layer within the Iceland Basin is probably due to mixing between ISOW and LSW in this density range. Some of the transport attributed to LSW between 27.70–27.85 kg m^{-3} is actually of a less dense form of ISOW or a mixture of LSW and ISOW. Around 70 % of the south-westward LSW transport occurs in the first 400 km of the EEL where south-westward flowing ISOW is predominantly found (Figure 10). Examination of data in θ-S space (Figure 5) shows the presence of higher salinity water existing at the same density level as the fresh LSW core. Further θ-S analysis (not shown) indicates that this is as a result of the influence of ISOW in the 27.70–27.85 kg m^{-3} density range. As such, the net ISOW layer transport estimate defined by isopycnals is likely to be an underestimate of the true south-westward flow of ISOW, and the LSW layer net transport an overestimate of LSW flow.

We report that the surprising result that the maximum mean overturning stream function in the Rockall Trough and the Iceland Basin are nearly identical in density and pressure coordinates (Figure 12). This implies that the horizontal shear dominates over water mass transformation here, and that result is consistent with the location of the section being east of the central subpolar gyre where most of the water mass transformation takes place. In the Iceland Basin the maximum overturning is 4.4 ± 2.0 Sv at 815 m, and in the Rockall Trough it is 3.0 ± 3.7 Sv at 1145 m. The Iceland Basin has overall larger transport, but as noted above, the Rockall Trough dominates the net variability.

We have shown that the mean velocity and transport fields estimated from the CTD sections are consistent with previous estimates and highlighted the regions with strongest variability. At present, the uncertainty of estimates from individual sections are too large to draw conclusions about temporal variability. This is a primary motivation for the OSNAP array, which will make direct measurements of velocity across the subpolar North Atlantic from 2014 to 2018. In the meantime, our continuing research is focussing on the use of historical sea surface height data from altimeter missions, combined with ship-based measurements, and new measurements from gliders, to extract a better resolved time series of velocity and transport with lower errors. Ongoing analysis of ADCP data collected on most cruises since 1996 will examine the character and mechanisms of the high variability regions identified in this study.

Acknowledgments
The Extended Ellett Line project is funded through NERC's National Capability program (NC) and supported by NERC's National Marine Facilities Sea Systems at the National Oceanography Centre (NOC). Data are available from www.bodc.ac.uk. N.P.H. is funded by NC and NERC Large Grant UK-OSNAP (Overturning in the Subpolar North Atlantic Program, grant number NE/K010875/1). J.F.R. and T.S. were funded by NC. S.F.G. and S.C. are funded by NC and NACLIM, a project of the European Union 7th Framework Program (FP7 2007–2013) under grant agreement 308299. C.J. is funded by NACLIM. We thank Claus Böning (GEOMAR) for generously providing the FLAME model output.

References

Beckmann, A., and R. Döscher (1997), A method for improved representation of dense water spreading over topography in geopotential coordinate models, *J. Phys. Oceanogr.*, *27*, 581–591.

Beszczynska-Möller, A. and S. R. Dye (Eds.) (2013), ICES Report on Ocean Climate 2012, *ICES Coop. Res. Rep. 321*, 73 pp., International Council for the Exploration of the Sea, Copenhagen, Denmark.

Beszczynska-Möller, A., E. Fahrbach, U. Schauer, and E. Hansen (2012), Variability in Atlantic water potential temperature and transport at the entrance to the Arctic Ocean, 1997–2010, *ICES J. Mar. Sci.*, *69*(5), 852–863, doi:10.1093/icesjms/fss056.

Böning, C. W., M. Scheinert, J. Dengg, A. Biastoch, and A. Funk (2006), Decadal variability of the subpolar gyre and its reverberation in the North Atlantic overturning, *Geophys. Res. Lett.*, *33*, L21S01, doi:10.1029/2006GL026906.

Brambilla, E., and L. D. Talley (2008), Subpolar mode water in the northeastern Atlantic: 1. Averaged properties and mean circulation, *J. Geophys. Res.*, *113*, C04025, doi:10.1029/2006JC004062.

Brambilla, E., L. D. Talley and P. Robbins (2008), Subpolar mode water in the northeastern Atlantic: 2. Origin and transformation, *J. Geophys. Res.*, *113*, C04026, doi:10.1029/2006JC004063.

Bryden, H. L., B. A. King, and G. McCarthey (2011), South Atlantic overturning circulation at 24°S, *J. Mar. Res.*, *69*(1), 38–55.

Burkholder, K. C., and M. S. Lozier (2011), Subtropical to subpolar pathways in the North Atlantic: Deductions from Lagrangian trajectories, *J. Geophys. Res.*, *116*, C07017, doi:10.1029/2010JC006697.

Chafik, L., T. Rossby, and C. Schrum (2014), On the spatial structure and temporal variability of poleward transport between Scotland and Greenland, *J. Geophys. Res. Oceans*, *119*, 824–841, doi:10.1002/2013JC009287.

Childers, K., C. Flagg, and T. Rossby (2014), Direct velocity observations of volume flux between Iceland and the Shetland Islands, *J. Geophys. Res. Oceans*, *119*, 5934–5944, doi:10.1002/2014JC009946.

Cunningham, S. A., and R. Marsh (2010), Observing and modelling changes in the Atlantic MOC, Wiley Interdisciplinary Reviews, *Clim. Change*, *1*(2), 180–191, doi:10.1002/wcc.22.

Desbruyeres, D., V. Thierry, and H. Mercier (2013), Simulated decadal variability of the meridional overturning circulation across the A25-Ovide section, *J. Geophys. Res. Oceans*, *118*, 462–475, doi:10.1029/2012JC008342.

Dickson, R. R., J. Meincke, S.-A. Malmberg, and A. J. Lee (1988), The "Great Salinity Anomaly" in the northern North Atlantic 1968–82, *Prog. Oceanogr.*, *20*, 103–151.

Döös, K. and D. Webb (1994), The Deacon Cell and other meridional cells of the Southern Ocean, *J. Phys. Oceanogr.*, *24*, 429–442.

Eldevik, T., J. E. O. Nilsen, D. Iovino, K. A. Olsson, A. B. Sando, H. Drange (2009), Observed sources and variability of Nordic seas overflow, *Nat. Geosci.*, *2*(6), 405–409, doi:10.1038/ngeo518.

Ellett, D., and K. Martin (1973), The physical and chemical oceanography of the Rockall Channel, *Deep Sea Res. Oceanogr. Abstr*, *20*, 585–625.

Ellett, D., A. Edwards, and R. Bowers (1986), The hydrography of the Rockall Channel: An overview, *Proc. R. Soc. Edinburgh*, *88B*, 61–81.

Gary, S. F., M. S. Lozier, C. W. Böning, and A. Biastoch (2011), Deciphering the pathways for the deep limb of the meridional overturning circulation, *Deep Sea Res., Part II*, *58*, 1781–1797, doi:10.1016/j.dsr2.2010.10.059.

Gary, S. F., M. S. Lozier, Y.-O. Kwon, and J. J. Park (2014), The fate of North Atlantic Subtropical Mode Water in the FLAME model, *J. Phys. Oceanogr.*, *44*, 1354–1371, doi:10.1175/JPO-D-13–0202.1.

Gourcuff, C., P. Lherminier, H. Mercier, and P. Le Traon (2011), Altimetry combined with hydrography for ocean transport estimation, *J. Atmos. Oceanic Technol.*, *28*, 1324–1337.

Glessmer, M. S., T. Eldevik, K. Vage, J. E. Nilsen, and E. Behrens (2014), Atlantic origin of freshwater anomalies in the Nordic Seas, *Nat. Geosci.*, *7*, 801–805.

Hakkinen, S., and P. B. Rhines (2004), Decline of subpolar North Atlantic circulation during the 1990s, *Science*, *304*(5670), 555–559.

Hakkinen, S., and P. B. Rhines (2009), Shifting surface currents in the northern North Atlantic Ocean, *J. Geophys. Res.*, *114*, C04005, doi: 10.1029/2008JC004883.

Hakkinen, S., P. Rhines, and D. Worthen (2011a), Atmospheric blocking and Atlantic multidecadal ocean variability, *Science*, *334*, 655–659, doi:10.1126/science.1205683.

Hakkinen, S., P. Rhines, and D. Worthen (2011b), Warm and saline events embedded in the meridional circulation of the northern North Atlantic, *J. Geophys. Res.*, *116*, C03006, doi:10.1029/2010JC006275.

Hansen, B., and S. Østerhus (2000), North Atlantic: Nordic seas exchanges, *Progr. Oceanogr.*, *45*, 109–208.

Hansen, B., S. Osterhus, H. Hatun, R. Kristiansen, and K. M. H. Larsen (2003), The Iceland-Faroe inflow of Atlantic water to the Nordic Seas, *Progr. Oceanogr.*, *59*(4), 443–474, doi:10.1016/j.pocean.2003.10.003.

Hátún, H., A. B. Sando, H. Drange, B. Hansen, and H. Valdimarsson (2005), Influence of the Atlantic subpolar gyre on the thermohaline circulation, *Science*, *309*, 1841–1844.

Heywood, K. J., E. L. McDonagh, and M. A. White (1994), Eddy kinetic energy of the North Atlantic subpolar gyre from satellite altimetry, *J. Geophys. Res.*, *99*, 22,525–22,539, doi:10.1029/94JC01740.

Holliday, N. P. (2003), Air-sea interaction and circulation changes in the northeast Atlantic, *J. Geophys. Res.*, *108*(C8), 3259, doi:10.1029/2002jc001344.

Holliday, N. P., and S. Cunningham (2013), The Extended Ellett Line: Discoveries from 65 years of marine observations west of the UK, *Oceanography*, *26*(2), 156–163, doi:10.5670/oceanog.2013.17.

Holliday, N. P., R. T. Pollard, J. F. Read, and H. Leach (2000), Water mass properties and fluxes in the Rockall Trough: 1975 to 1998, *Deep Sea Res., Part I*, *47*,(7), 1303–1332.
Holliday, N. P., M. J. Yelland, R. Pascal, V. R. Swail, P. K. Taylor, C. Griffiths, and E. C. Kent (2006), Were extreme waves in the Rockall Trough the largest ever recorded?, *Geophys. Res. Lett.*, *33*, L05613, doi:10.1029/2005GL025238.
Holliday, N. P., et al. (2008), Reversal of the 1960s to 1990s freshening trend in the northeast North Atlantic and Nordic Seas, *Geophys. Res. Lett.*, *35*, L03614, doi:10.1029/2007GL032675.
Hughes, S. L., N. P. Holliday, and F. Gaillard (2012), Variability in the ICES/NAFO region between 1950 and 2009: Observations from the ICES Report on Ocean Climate, *ICES J. Mar. Sci.*, *69*(5), 706–719, doi:10.1093/icesjms/fss044.
Inall, M. E., P. A. Gillibrand, C. Griffiths, N. MacDougall, and K. Blackwell (2009), On the oceanographic variability of the North-West European Shelf to the West of Scotland, *J. Mar. Syst.*, *77*, 210–226, doi:10.1016/j.jmarsys.2007.12.012.
Johnson, C., T. Sherwin, D. Smythe-Wright, T. Shimmield, and W. Turrell (2010), Wyville Thomson Ridge Overflow Water: Spatial and temporal distribution in the Rockall Trough, *Deep Sea Res., Part I*, *57*(10), 1153–1162, doi:10.1016/j.dsr.2010.07.006.
Johnson, C., M. E. Inall, and S. Hakkinen (2013), Declining nutrient concentrations in the northeast Atlantic as a result of a weakening Subpolar Gyre, *Deep Sea Res., Part I*, *82*, 95–107, doi:10.1016/j.dsr.2013.08.007.
Jonsson, S., and J. Briem (2003), Flow of Atlantic water west of Iceland and onto the north Icelandic shelf, *ICES Mar. Sci. Symp.*, *219*, 326–328.
Kalnay, E. M. et al. (1996), The NCEP/NCAR 40-year reanalysis project, *Bull. Am. Meteorol. Soc.*, *77*, 437–471, doi:10.1175/1520-0477(1996)077<0437:TNYRP>2.0.CO;2.
Kanzow, T., and W. Zenk (2014), Structure and transport of the Iceland Scotland Overflow plume along the Reykjanes Ridge in the Iceland Basin, *Deep Sea Res. Part I*, *86*, 82–93.
Kuhlbrodt, T., A. Griesel, A., M. Montoya, A. Levermann, M. Hofmann, and S. Rahmstorf (2007), On the driving processes of the Atlantic Meridional Overturning Circulation, *Rev. Geophys.*, *45*, RG2001, doi:10.1029/2004RG000166.
Lankhorst, M., and W. Zenk (2006), Lagrangian observations of the mid depth and deep velocity fields of the northeastern Atlantic Ocean, *J. Phys. Oceanogr.*, *36*(1), 43–63.
Lavender, K. L., W. B. Owens, and R. E. Davis (2005), The mid-depth circulation of the subpolar North Atlantic Ocean as measured by subsurface floats, *Deep Sea Res., Part I*, *52*, 767–785.
Lherminier, P., H. Mercier, C. Gourcuff, M. Alvarez, S. Bacon, and C. Kermabon (2007), Transports across the 2002 Greenland-Portugal Ovide section and comparison with 1997, *J. Geophys. Res.*, *112*, C07003, doi:10.1029/2006JC003716.
Lherminier, P., H. Mercier, T. Huck, C. Gourcuff, F. F. Perez, P. Morin, A. Sarafanov, and F. Anastasia (2010), The Atlantic Meridional Overturning Circulation and the subpolar gyre observed at the A25-OVIDE section in June 2002 and 2004, *Deep Sea Res. Part I*, *57*(11), 1374–1391, doi:10.1016/j.dsr.2010.07.009.
Lozier, M. S., and N. M. Stewart (2008), On the temporally varying northward penetration of Mediterranean Overflow Water and eastward penetration of Labrador Sea water, *J. Phys. Oceanogr.*, *38*(9), 2097–2103, doi:10.1175/2008JPO3908.1.
Østerhus, S., W. Turrell, B. Hansen, P. Lundberg, and E. Buch (2001), Observed transport estimates between the North Atlantic and the Arctic Mediterrranean in the Iceland-Scotland region, *Polar Res.*, *20*, 169–175.
Pollard, R. T., J. F. Read, N. P. Holliday, and H. Leach (2004), Water masses and circulation pathways through the Iceland Basin during Vivaldi 1996, *J. Geophys. Res.*, *109*, C04004, doi:10.1029/2003JC002067.
Polyakov, I.V., et al. (2011), Fate of early 2000s Arctic warm water pulse, *Bull. Am. Meteorol. Soc.*, *92*(5), 561–566, doi:10.1175/2010BAMS2921.1.
Read, J. F. (2001), CONVEX-91: Water masses and circulation of the Northeast Atlantic subpolar gyre, *Progr. Oceanogr.*, *48*, 461–510.
Rio, M. H., S. Guinehut, and G. Larnicol (2011), New CNES-CLS09 global mean dynamic topography computed from the combination of GRACE data, altimetry, and in situ measurements, *J. Geophys. Res.*, *116*, C07018, doi:10.1029/2010JC006505.
Sarafanov, A., A. Falina, H. Mercier, A. Sokov, P. Lherminier, C. Gourcuff, S. Gladyshev, F. Gaillard, and N. Daniault, (2012), Mean full-depth summer circulation and transports at the northern periphery of the Atlantic Ocean in the 2000s, *J. Geophys. Res.*, *117*, C01014, doi:10.1029/2011JC007572.
Saunders, P. (1996), The flux of dense cold overflow water southeast of Iceland, *J. Phys. Oceanogr.*, *26*, 85–95.
Stentardo, I., D. Keike, M. Rhein, N. Gruber, and R. Steinfelt (2015), Interannual to decadal oxygen variability in the mid-depth water masses of the eastern North Atlantic, *Deep Sea Res., Part I*, *95*, 85–98, doi:10.1016/j.dsr.2014.10.009.
Stommel, H. (1961), Thermohaline convection with two stable regimes of flow, *Tellus*, *13*, 224–230.
Turrell, B., B. Hansen, S. L. Hughes, and S. Osterhus (2003), Hydrographic variability during the decade of the 1990s in the Northeast Atlantic and southern Norwegian Sea, *ICES Mar. Sci. Symp.*, *219*, 111–120.
Yashayaev, I., M. Bersch, and H. van Aken (2007a), Spreading of the Labrador Sea water to the Irminger and Iceland basins, *Geophys. Res. Lett.*, *34*(10), L10602, doi:10.1029/2006GL028999.
Yashayaev, I., H. M. van Aken, N. P. Holliday, and M. Bersch (2007b), Transformation of the Labrador Sea water in the subpolar North Atlantic, *Geophys. Res. Lett.*, *34*, L22605, doi:10.1029/2007GL031812.